Ore Geology Reviews 76 (2016) 229–256

Contents lists available at ScienceDirect

Ore Geology Reviews

journal homepage: www.elsevier.com/locate/oregeorev

Radiogenic isotopes, ore deposits and metallogenic terranes: Novel approaches based on regional isotopic maps and the mineral systems concept

David C. Champion *, David L. Huston

Geoscience Australia, GPO Box 378, Canberra, ACT, 2601, Australia

ARTICLE INFO

Article history:
Received 3 December 2014
Received in revised form 11 September 2015
Accepted 23 September 2015
Available online 26 September 2015

Keywords:
Mineral systems,
Radiogenic isotopes,
Sm–Nd
U–Th–Pb,
Metallogenesis,
Ore deposits,
Metallogenic terranes

ABSTRACT

Radiogenic isotopes have long been used in mineralisation studies, not just for geochronological determinations of mineralising events but also as tracers, providing, for example, information on the source of metals. It was also evident early on that consideration of isotopic data on a regional scale could be used to assist with metallogenic interpretation, including identification of metallogenic terranes. The large amounts of isotopic (and other) data available today, in combination with readily available graphical software, have made possible construction of isotopic maps, using various isotopic variables, at regional to continental scales, allowing for metallogenic interpretation over similarly large regions. Such interpretation has been driven largely by empiricism, but increasingly with a mineral systems approach, recognising that mineral deposits, although geographically small in extent, are the result of geological processes that occur at a variety of scales.

This review looks at what radiogenic isotopes can tell us about different mineral systems, from camp- to craton-scale. Examples include identifying lithospheric/crustal architecture and its importance in controlling the locations of mineralisation, the identification of metallogenic terranes and/or favourable geodynamic environments on the basis of their isotopic signatures, and using juvenile isotopic signatures of intrusives to identify metallogenically important rock types. The review concentrates on the Sm–Nd system using felsic igneous rocks and the U–Th–Pb system using galena, Pb-rich ores and other rocks. The Sm–Nd system can be used to effectively 'see' through many crustal processes to provide information on the nature of the source of the rocks. For voluminous rocks such as granites this provides a potentially powerful proxy in constraining the nature of the various crustal blocks the granites occur within. In contrast, Pb isotopic data from galena and Pb-rich associated ores provide a more direct link to mineralisation, and the two systems (Pb and Nd) can be used in conjunction to investigate links between mineralisation and crustal domains.

In this contribution we document: the more general principles of radiogenic isotopes; the identification of time-independent isotopic parameters; the use of such variable to generate isotopic maps, and the use of the latter for metallogenic studies. Regional and continental scale isotopic maps (and data) can be used to empirically and/or predictively to identify and target (either directly or indirectly by proxy) larger scale parts of mineral systems that may be indicative of, or form part of metallogenic terranes. These include demonstrable empirical relationships between mineral systems and isotopic domains, which can be extracted, tested and applied as predictive tools. Isotopic maps allow the identification of old, especially Archean, cratonic blocks, which may be metallogenically-endowed, or have other favourable characteristics. These maps also assist with identification of potentially favourable paleo-tectonic settings for mineralisation. These include: old continental margins, especially accretionary orogenic settings; and juvenile zones, either marginal or internal, which may indicate extension and possible rifting, or primitive arc crust. Such isotopic maps also aid identification of crustal breaks, which may represent major faults zones and, hence, fluid pathways for fluids and magmas, or serve to delineate natural boundaries for metallogenic terranes. Finally, isotopic maps also act as baseline maps which help to identify regions/periods characterised by greater (or lesser) magmatic, especially mantle input. Of course, in any exploration model, any analysis is predicated on using a wide range of geological, geochemical and geophysical information across a range of scales. Sm–Nd and U–Th–Pb isotopic maps are just another layer to be integrated with other data. Future work should focus on better constraining the 4D (3D plus time) evolution of the lithosphere, by integrating isotopic data with other data, as well as through better integration of available radiogenic isotopic systems, including the voluminous amounts of in situ isotopic analysis (of minerals) now available. This should result in more effective commodity targeting and exploration.

* Corresponding author.
E-mail address: David.Champion@ga.gov.au (D.C. Champion).

http://dx.doi.org/10.1016/j.oregeorev.2015.09.025
0169-1368/

1. Introduction

Radiogenic isotopes have long been used in mineralisation studies, not just for geochronological determinations of mineralisation but also commonly as tracers, i.e. to provide information on geological processes and the components involved in such processes. Isotopes can provide information on the nature, age and source of mineralisation, the pathways of fluids, possible metal sources, and on the processes responsible for mineralisation, and there is a voluminous literature regarding the use of radiogenic isotopes, including a number of review papers (e.g., Tosdal et al., 1999; Lambert et al., 1999; Ruiz and Mathur, 1999, and references therein). It was recognised many years ago that regional-scale isotopic maps could be generated and used to assist with metallogenic interpretation and identification of metallogenic terranes (e.g., Zartman, 1974; Farmer and DePaolo, 1984; Wooden et al., 1998). Today large amounts of isotopic (and other) data are available and are being produced at an ever increasing rate. These data, in combination with readily available graphical software, have made possible construction of isotopic maps, using various isotopic variables, at regional to continental scales. Examples include Cassidy et al. (2002), Champion and Cassidy (2007, 2008), Champion (2013), Huston et al. (2014), and Mole et al. (2013) for the Sm–Nd system, Huston et al. (2014, 2016-in this volume) for the Pb system and Mole et al. (2014) for the Lu–Hf system. These include the first continental-scale isotopic map, produced by Champion (2013) for the Australian continent.

The usefulness of such isotopic maps for metallogenic studies has also become increasingly apparent since pioneering studies such as Zartman (1974). This has been driven largely by empiricism, e.g., Zartman (1974), Wooden et al. (1998), Cassidy and Champion (2004), Cassidy et al. (2005), Huston et al. (2005, 2014), but increasingly by the development and application of a mineral systems approach (Huston et al., 2016-in this volume). Mineral deposits form through the coincidence of favourable geological processes within a given spatial setting and commonly at a specific geological time. Like the petroleum system concept (Magoon and Dow, 1994), an analogous mineral system concept can also be defined, encompassing "all geological factors that control the generation and preservation of mineral deposits" (Wyborn et al., 1994). Although there are a variety of interpretations of what a mineral system is (e.g., Wyborn et al., 1994; Barnicoat, 2007; McCuaig et al., 2010; Huston et al., 2012; see Fig. 1), most include factors such as the geological setting, the timing and duration of deposition, the source(s) and nature of mineralising fluids (including magmas), the pathways utilised by the respective fluid and fluid flow drivers, the depositional site, mechanisms of metal transport and deposition, and post-depositional modifications (Fig. 1A). The mineral systems concept, e.g., Wyborn (1997), recognises that mineral deposits, although geographically small in extent, are the result of geological and geodynamic processes that occur, and can be mapped at, a variety of larger scales (Fig. 1; e.g., McCuaig et al., 2010; Hronsky et al., 2012). Accordingly, a better knowledge of the space-time evolution of geological terranes and their components provides important constraints on prior geodynamic regimes and lithospheric architectures which may have played an important role in mineral systems. This increased understanding has the potential to explain the often heterogeneous distribution of mineralisation within regions. A good example of this are models for the generation of the strong Ni-endowment present within the Norseman-Wiluna belt, Eastern Goldfields Superterrane (EGST), Yilgarn Craton, Western Australia (e.g., Begg et al., 2010; Barnes and Fiorentini, 2010a, 2010b, 2012; Mole et al., 2014), which implicate a strong role for pre-existing lithosphere architecture in controlling fluid flow (in this case ultramafic magmas) and pathways and the location of komatiitic nickel deposits. This example highlights an important point regarding the mineral systems approach as used here, namely that important controls on mineralisation may have been in place prior to the mineralisation event.

Just as the mineral system works over a range of scales so too does the applications for radiogenic isotopes. At the larger scale (camp- to continent-scale), radiogenic isotopes have the potential to inform on the architecture of the system and the geological framework, i.e., on the geodynamic and geological history of the lithosphere the respective deposit occurs in. It is at these scales that regional isotopic maps are at their most useful and informative. This review, therefore, looks at what radiogenic isotopes can tell us about different mineral systems, particularly focussing on their use for mineral systems at the craton- to camp-scale. Examples include: identifying lithospheric/crustal architecture and its importance in controlling the locations of mineralisation; the identification of metallogenic terranes and/or favourable geodynamic environments on the basis of isotopic signatures; and identifying metallogenically important rock types by their isotopic signature.

The paper concentrates on the Sm–Nd and U–Th–Pb isotopic systems, which have been in use for a long period (e.g., Zartman, 1974; Farmer and DePaolo, 1983, 1984; Bennett and DePaolo, 1987), and for which the most comprehensive regional isotopic data are available. We document the general principles of radiogenic isotopes; the identification of time-independent isotopic variables; the use of such variable to generate isotopic maps, and the use of the latter for metallogenic studies. Examples from other systems (Lu–Hf, Re–Os) are also included, particularly coupled isotopic systems, which provide additional constraints on the links between lithospheric processes and mineralisation.

2. Mineral systems and radiogenic isotopes

The multi-scale mineral systems approach means that knowledge of the four-dimensional evolution of any geological terrane is important for both a better understanding of metallogeny and for more efficient mineral exploration (e.g., McCuaig et al., 2010). A better understanding of the four-dimensional evolution of any geological terrane encompasses a greater knowledge of the lithosphere of that terrane, including not just the more readily mappable upper crust but the more inaccessible lower crust and mantle lithosphere components (Fig. 1B). This is where radiogenic isotopes are most useful as they can supply not just potential ages of these regions but also constraints on their nature, such as their composition and how they may have formed. This is particularly the case when applied to rocks that may have either formed in the lower crust or mantle lithosphere, or have interacted with these regions. A good example of this approach is the extensive work over many decades on the characterisation of the asthenosphere on the basis of isotope systematics and geochemistry of basalts and other mantle-derived rocks (e.g., Zindler and Hart, 1986). A similar approach can be used to constrain crustal evolution by using the isotopic (and geochemical and geochronological) characteristics of granites and other felsic igneous rocks, as has been done in the western United States (e.g., Zartman, 1974; Farmer and DePaolo, 1983, 1984; Bennett and DePaolo, 1987; Wooden et al., 1998). Because such rocks are dominantly derived from the (lower-middle) continental crust, usually in significant volumes (e.g., granite plutons can have volumes in the order of tens to hundreds of km^3), these rocks provide direct constraints on the timing, extent and nature of crustal growth. Studies of felsic igneous rocks also provide important, but less precise, indirect constraints on the nature and age of the crustal domains these rocks occur within (e.g., Farmer and DePaolo, 1983, 1984).

Another approach to constraining the crustal evolution of a metallogenic province is to use geochemical characteristics of the mineral deposits. Like granites, the geochemical and isotopic characteristics of a mineral deposit, in part, reflect their source which, depending upon the specific mineral system can be the mantle and all parts of the crust. Like granite, the geochemical and isotopic characteristics of a mineral deposit are averages of the sources that can be affected, in many cases fundamentally, by processes that occur at the site of mineralisation. However, despite these complexities, isotopic mapping using data

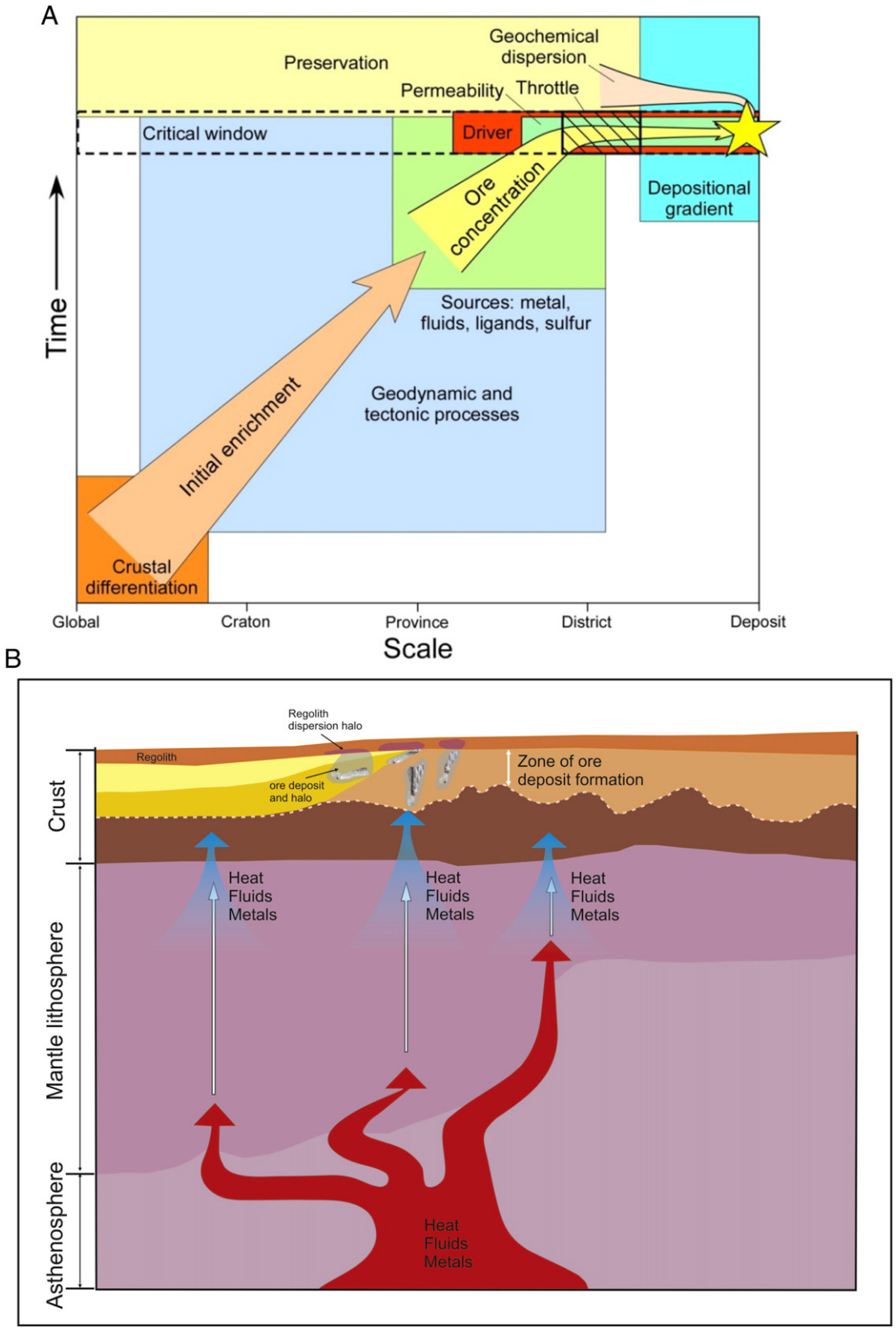

Fig. 1. Mineral system models and examples. A) Mineral system model illustrating the range of processes required to produce a mineral deposit. Such processes operate at a range of spatial and temporal scales. Model developed by Huston et al. (2015). B) Cartoon illustrating a number of potential processes that may be important for a specific mineral deposit, illustrating the large range of scales processes operate over relative to the scale of the deposit. Figure modified from 'Searching the Deep Earth' (http://www.science.org.au/policy/documents/uncover-report.pdf).

from mineral deposits—in particular Pb (e.g., Zartman, 1974; Carr et al., 1995; Huston et al., 2016-in this volume), but also other isotopic systems—can yield information that is complementary to isotopic mapping using granites as the medium. Johnson and McCulloch (1995), for example, utilised the Nd isotopic signature of ores to identify both mantle and crustal contributions to the Olympic Dam deposit.

How isotopic systems behave and the interpretation of isotopic data, is largely a function of the geochemical behaviour of both the parent and the daughter isotope, especially the relative behaviour of each, i.e., the fractionation of the daughter from the parent (Table 1). Individual radiogenic isotope systems (e.g., U–Th–Pb, Sm–Nd, Rb–Sr, Re–Os, Lu–Hf) therefore, can provide differing (often complementary) constraints on geological processes, geological reservoirs (e.g., mantle, crust), and rock types, e.g., mafic or felsic igneous rocks. For the study of felsic igneous rocks a range of isotopic systems have been used (e.g., Pb—Wooden et al., 1998; Sr—Farmer and DePaolo, 1983), though it is the Sm–Nd (e.g., Farmer and DePaolo, 1983, 1984; Bennett and DePaolo, 1987), and more recently Lu–Hf (e.g., Kemp et al., 2007; Mole et al., 2014) systems that have been most commonly used for studying granite petrogenesis and making inferences regarding crust and mantle sources. Of these, the former has been routinely analysed for more than 30 years providing a wealth of available data. It is a well understood relatively simple system coupled with a number of features that make it applicable for felsic igneous rocks and for constraining crustal evolution (see DePaolo, 1988).

For the Sm–Nd system, both parent and daughter isotopes are members of the lanthanide series of elements—also known as the rare earth elements (REE)—which all have very similar geochemical properties. As such they exhibit similar, generally predictable, geochemical behaviour for most geological processes, e.g., the formation of felsic igneous rocks such as granites. As a result of this similar behaviour there is generally only minor fractionation between the two elements, i.e., the Sm/Nd ratio does not greatly vary in common crustal rocks (see Table 2). What fractionation that does occur is largely related to another property of the REE, namely lanthanide contraction, whereby successively heavier lanthanides (higher atomic number) have increasingly smaller atomic radii. This means that lighter REE, such as Nd, behave (albeit only slightly) more incompatibly than heavier REE, such as Sm. As a result, many geological processes, such as partial melting and fractional crystallisation, almost always result in not just higher concentrations of the light REE (LREE) but also lower Sm/Nd ratios in the more siliceous end-members (see, for example, modelling in DePaolo, 1988).

A clear result of the effect of lanthanide contraction on incompatibility can be seen in the chemical zonation of the earth. The earth's crust is not only more enriched in the lighter REE such as Nd and Sm, but also has correspondingly lower Sm/Nd ratios than the complementary depleted mantle reservoir. As pointed out by many workers (e.g., DePaolo and Wasserburg, 1976; Bennett and DePaolo, 1987; see discussion in DePaolo, 1988), the differing Sm/Nd ratios of mantle and crustal reservoirs result in markedly different time integrated behaviour through time (Table 2; Fig. 2).

Table 2
Average Nd, Sm, Pb, Th and U concentrations (in parts-per-million) and Sm/Nd and U/Pb ratios of mantle and crustal reservoirs. Sources: continental crust reservoirs from Rudnick and Gao (2004), mid-ocean ridge basalt (MORB) from Arevalo and McDonough (2010); ocean island basalt (OIB), enriched- and depleted MORB (EMORB and NMORB) from Sun and McDonough (1989); depleted mantle from Salters and Stracke (2004); bulk earth and core from McDonough (2003), silicate earth from McDonough and Sun (1995), C1 carbonaceous chondrite from Palme and Jones (2003).

Reservoir	Nd	Sm	Sm/Nd	Pb	Th	U	U/Pb
Upper crust	27	4.7	0.17	17	10.5	2.7	0.16
Middle crust	25	4.6	0.18	15.2	6.5	1.3	0.09
Lower crust	11	2.8	0.26	4	1.2	0.2	0.05
Bulk crust	20	3.9	0.20	11	5.6	1.3	0.12
OIB	38.5	10.0	0.26	3.2	4.0	1.02	0.32
MORB	9.8	3.25	0.26	0.57	0.219	0.080	0.32
E-MORB	9.0	2.6	0.29	0.6	0.6	0.18	0.30
N-MORB	7.3	2.63	0.36	0.3	0.12	0.047	0.16
Depleted mantle	0.71	0.27	0.38	0.023	0.014	0.005	0.22
Silicate earth	1.25	0.41	0.33	0.15	0.08	0.02	0.13
Bulk earth	0.84	0.27	0.32	0.23	0.055	0.015	0.065
Core	0	0		0.4	0	0	
Chondrite	0.474	0.154	0.32	2.53	0.0298	0.0078	0.003

The Sm–Nd system also has another feature—the very long half-life of ^{147}Sm (106 billion years)—which when combined with those highlighted above, make the system ideal for studying crustal development. Namely, significant changes in the Nd isotopic signature require either long time frames to develop and/or require significant fractionation of the Sm/Nd ratio (such as juvenile crustal growth) and/or addition of isotopically distinct end-members (e.g., for granites the incorporation of a juvenile mantle component). As documented by DePaolo (1988), this behaviour means that the Sm–Nd system can be used to effectively 'see' through many crustal processes and can provide information on the nature of the source of the rocks in question. For voluminous rocks such as granites, which commonly have a significant crustal component, this provides a potentially powerful proxy in constraining the nature of the various crustal blocks the granites occur within, i.e., in effect broadly mapping the crust and crustal growth as demonstrated by Bennett and DePaolo (1987).

In comparison with Sm and Nd, which have similar geochemical properties, the geochemical properties of U, Th and Pb are more variable. Although all three elements tend to concentrate in the crust, especially the upper continental crust (Rudnick and Gao, 2004),

Table 1
Some important radiogenic isotope systems, detailing parent and daughter isotopes, half lives (and lambda values), stable isotope, and comments on geochemical behaviour of parent and daughter. Half lives and λ values from Dickin (1995), except for Lu–Hf which is from Söderlund et al. (2004), and Re–Os from Carlson (2005).

System	Parent isotope	Daughter isotope	$t^{1/2}$ (Ga) λ	Stable isotope	Comments
Sm–Nd	^{147}Sm	^{143}Nd	106 6.54×10^{-12}	^{144}Nd	Both parent and daughter are light rare earth elements and have lithophile behaviour. Both behave very similarly, and are concentrated in the upper continental crust. $^{143}Nd/^{144}Nd$ often reported as ε_{Nd}. Commonly also reported with depleted mantle model ages.
U–Pb	^{238}U	^{206}Pb	4.47 1.55125×10^{-10}	^{204}Pb	U lithophile, Pb lithophile and chalcophile; both concentrated in upper continental crust; Pb preferentially concentrated in many mineral deposits. Often reported as $^{206}Pb/^{204}Pb$ and $^{207}Pb/^{204}Pb$ ratios; also as μ values ($^{238}U/^{204}Pb$), and model ages based on these values (and $^{207}Pb/^{204}Pb$ and $^{206}Pb/^{204}Pb$).
	^{235}U	^{207}Pb	0.704 9.8485×10^{-10}	^{204}Pb	
Th-Pb	^{232}Th	^{208}Pb	14.01 0.49475×10^{-10}	^{204}Pb	Th lithophile, Pb lithophile and chalcophile; both concentrated in upper continental crust; Pb preferentially concentrated in many mineral deposits. Often reported as $^{208}Pb/^{204}Pb$ ratios.
Re–Os	^{187}Re	^{187}Os	42.3 1.666×10^{-11}	^{186}Os	Both siderophile. Re is preferentially concentrated in mantle melts (and crust) relative to Os, giving high Re/Os ratios in such melts. Os mostly resident in the (depleted) mantle and core; Re is more evenly distributed. $^{187}Os/^{186}Os$ also reported as γ_{Os}, and also Re–Os mantle model ages (T_{MA}) and Re-depletion model ages (T_{RD}) (see Carlson, 2005).
Lu–Hf	^{176}Lu	^{176}Hf	37.1 1.867×10^{-11}	^{177}Hf	Both are lithophile, and behave as high-field strength elements. Lu—a rare earth element—is concentrated within mantle melts and the crust; Hf is concentrated in the upper continental crust and commonly follows Zr. $^{176}Hf/^{177}Hf$ often reported as ε_{Hf}. Often also reported with depleted mantle model ages. The majority of modern analyses are measured using the mineral zircon (which has very low Lu/Hf ratios).
Rb–Sr	^{87}Rb	^{87}Sr	48.8 1.42×10^{-11}	^{86}Sr	Both parent and daughter are lithophile, Rb is concentrated in middle and upper continental crust, Sr is more evenly distributed, leading to significant changes in Rb/Sr from lower to upper crust.

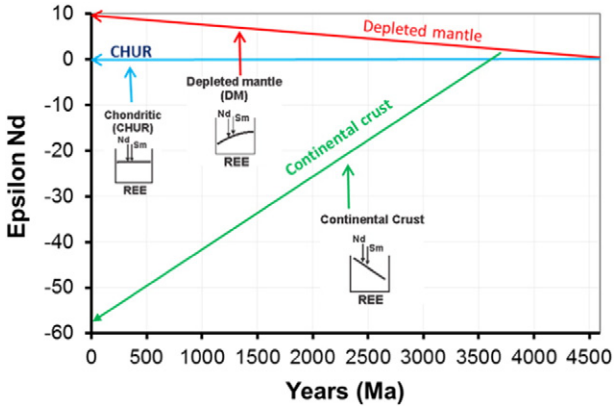

Fig. 2. Time integrated behaviour of ε_{Nd} in continental crustal reservoirs versus the complementary depleted mantle reservoir. Small REE plots illustrate the idealised change in Sm/Nd ratio (normalised to Chondrite) between the reservoirs. CHUR equals Chondritic Uniform Reservoir.

following Goldschmidt's classification, U and Th are lithophile (rock-loving) elements whilst Pb is a chalcophile element (sulphur-loving). This leads to substantially different geochemical behaviours within the crust (and mantle and core; Table 2) and the development of isotopically diverse and provincial source reservoirs. Although these differences in behaviour require more complex, and thereby often less robust, models for isotopic evolution than, for example the Sm–Nd system, Pb isotopic data can be used to map crustal structures, and does correlate with inferences based from other isotopic systems, as shown by Wooden et al. (1998). Moreover, Pb can be commonly strongly fractionated from U and Th in many crustal processes such as mineralisation, producing Pb-rich and U- and Th-poor rocks and minerals (e.g., galena) that retain and directly constrain initial isotopic ratios. We concentrate here on Pb isotopic data from galena and Pb-rich associated ores and other rocks, as these provide a more direct link between mineralisation, and various isotopic domains, as delineated by Pb and other (e.g., Sm–Nd) isotopic data.

3. Radiogenic isotope principles

There are many review papers and books written on isotope systematics (e.g., Faure, 1977; DePaolo, 1988; Dickin, 1995) and readers are referred to them for detailed discussion of each isotopic system; only a very general introduction is provided here, using Sm–Nd as the main example, and the U–Th–Pb system as a secondary example. Radiogenic isotopes are derived by the decay (at a constant decay rate = λ) of a radioactive parent to a more stable daughter isotope, e.g., ^{147}Sm radioactively decays to the radiogenic ^{143}Nd isotope, emitting an alpha particle ($^{147}Sm \rightarrow {}^{143}Nd + \alpha$); see Table 1 for others. The amount of daughter isotope produced by radioactive decay from the parent isotope is a function of the half-life of the parent isotope and the time, in years, the parent has been decaying:

$$(\text{Daughter}) = (\text{parent isotope}) * \left(e^{\lambda t} - 1\right) \quad (1)$$

where t = the period of time in question, and λ = the decay constant (proportional to the reciprocal of the half-life; see Table 1).

The amount of daughter isotope present in any rock is the sum of the initial daughter isotope concentration, plus the amount of the daughter isotope produced over time from the decay of the parent isotope:

$$(\text{Daughter isotope})_{(\text{now})} = (\text{Daughter})_{(\text{initial})} + (\text{parent isotope})_{(\text{now})} * \left(e^{\lambda t} - 1\right) \quad (2)$$

where: (now) = abundance of the isotope as measured in the present day, (initial) = abundance of the isotope at time t in the past, and t = the age (in years) of the rock, (e.g., the magmatic, metamorphic, or mineralisation age).

Analytical results for parent and daughter are commonly reported relative to a stable (non-radiogenic) isotope (for Sm–Nd this is ^{144}Nd). The evolution of these ratios through time (in a closed system) is as follows:

$$\left(^{143}Nd/^{144}Nd\right)_{(\text{now})} = \left(^{143}Nd/^{144}Nd\right)_{(\text{initial})} + \left(^{147}Sm/^{144}Nd\right)_{(\text{now})} * \left(e^{\lambda t} - 1\right). \quad (3)$$

Equations such as these are commonly used for determining the age of rocks (e.g., see Faure, 1977). For tracer applications, the initial parent/daughter ratio (initial ratio) is commonly more important and equations such as Eq. 4) are used.

$$\left(^{143}Nd/^{144}Nd\right)_{(\text{initial})} = \left(^{143}Nd/^{144}Nd\right)_{(\text{now})} - \left(^{147}Sm/^{144}Nd\right)_{(\text{now})} * \left(e^{\lambda t} - 1\right). \quad (4)$$

For a variety of reasons, including the fact that many isotopic ratios are measured to many decimal places (required because of the long half-lives, e.g., the 106 Ma half-life of ^{147}Sm means deviations in $^{143}Nd/^{144}Nd$ are small, typical in the 4th and 5th decimal places), initial ratios are often reported using other notation, usually as deviations from some model earth reservoir (see Table 1). For example, $^{143}Nd/^{144}Nd$ values are commonly reported as epsilon (ε) units (DePaolo and Wasserburg, 1976), which are deviations in part per ten thousand from a chondritic earth reference model (CHUR = Chondritic Uniform Reservoir), as follows:

$$\varepsilon_{Nd} = 10,000 * \left[\left(^{143}Nd/^{144}Nd\right)_{\text{Sample(T)}} - \left(^{143}Nd/^{144}Nd\right)_{\text{CHUR(T)}}\right] / \left(^{143}Nd/^{144}Nd\right)_{\text{CHUR(T)}}. \quad (5)$$

Sm–Nd data are typically displayed using ε_{Nd}-time plots. As with most radiogenic isotope systems, although mantle and crustal reservoirs tend to occupy different parts of such diagrams, this is not universal.

The U–Th–Pb isotopic system has many similarities but important differences to the Sm–Nd system described above. Like the latter, initial Pb isotopic ratios are most useful in understanding crustal processes. Unlike the Sm–Nd system, isotopic ratios in the U–Th–Pb system are commonly reported as the daughter Pb isotopes relative to the non-radiogenic isotope ^{204}Pb (Table 1), i.e., $^{206}Pb/^{204}Pb$, $^{207}Pb/^{204}Pb$ and $^{208}Pb/^{204}Pb$ (^{206}Pb and ^{207}Pb are uranogenic isotopes (derived from ^{238}U and ^{235}U, respectively) whereas ^{208}Pb is thorogenic (derived from ^{232}Th). These ratios are generally plotted as scattergrams against each other, with more juvenile and less juvenile reservoirs occupying different parts of the diagrams (e.g., Zartman, 1974). An important aspect of the U–Th–Pb system is that Pb-rich ore samples, e.g., galena or whole rocks with Pb greater than ~1000 ppm, can 'lock-in' initial ratios which are indicative of the ratios in the source reservoir at the time of extraction, i.e., the initial concentration of the respective daughter isotopes are so high relative to the parent isotopes (very low parent/daughter ratio) that there is very little time-integrated change in the isotopic signature. This is similar to Lu–Hf analysis of the mineral zircon which is essentially recording the $^{176}Hf/^{177}Hf$ composition at the time of zircon growth (e.g., Kemp et al., 2007).

3.1. Model ages and other isotopic parameters

Although initial ratios (and related measures, such as ε_{Nd}) are clearly important, especially when comparing rocks of roughly similar ages (e.g., initial $^{206}Pb/^{204}Pb$ in feldspars from felsic magmatic rocks in the

Nevada region (Wooden et al., 1998), initial $^{87}Sr/^{86}Sr$ ratios in Cenozoic basalts of southeastern Australia, Price et al., 2014), the time factor used in equations for their calculation means that they are difficult to use comparatively when looking at rocks of quite different ages, particularly for spatial comparisons. For example, consider two granites of vastly different age and vastly different negative ε_{Nd} values—it is difficult to make any conclusions regarding what they may be telling you about the relative isotopic signature of the crust they're in, let alone additional possible constraints on the relative nature of the crust. These difficulties can be minimised in a number of ways, typically by calculation of some model variable, e.g., calculation of μ (= mu) values for U-Pb systems, or via calculation of various model ages (Table 1). Isotopic systems have long been used to calculate model ages, i.e., the age when the isotope characteristics of the rock in question matched those of some modelled reservoir. This is one of the simplest ways to compare isotopic data from rocks of different age for the Sm–Nd system. The well understood behaviour of Sm and Nd, in combination with the observation for distinctly different time integrated behaviour of Nd isotopic signatures between mantle and crustal reservoirs (Fig. 2), led to the early recognition of the usefulness of Sm–Nd data for providing model age estimates for the age of continental crust in a region (e.g., McCulloch and Wasserburg, 1978; DePaolo, 1981, 1988; Farmer and DePaolo, 1983, 1984; Liew and McCulloch, 1985; Bennett and DePaolo, 1987; McCulloch, 1987; Fig. 3). Calculated Nd model ages effectively provide a simplistic estimate of the time a sample (=proxy for the crust in a region) has been separated from its (modelled) mantle source, typically depleted mantle. This approach is most useful for magmatic rocks, especially felsic magmatic rocks, but has been used for all rock types (McCulloch and Wasserburg, 1978).

Although early model ages were calculated assuming a chondritic mantle (T_{CHUR}), most are now calculated assuming depleted mantle (T_{DM}; DePaolo, 1981, 1988), with supra-chondritic Sm/Nd ratios (see discussion in Liew and McCulloch, 1985). A variety of models are used for depleted mantle. These include the DePaolo (1981) model which assumes an increasingly depleted mantle (calculated by $\varepsilon_{Nd(T)} = 0.25*T^2 - 3T + 8.5$; T in Ga); and the linear depletion model (the one used here) which assumes linear depletion from $\varepsilon_{Nd} = 0$ at ~4.56 Ga to +10 today (Fig. 3). McCulloch (1987), in his study of Australia, also assumed a linear model but assumed depletion commenced at 2.75 Ga. The linear depletion model gives slightly older model ages than the others. Model ages can also be calculated assuming single stage or multi-stage (typically two-stage) models. Single stage models

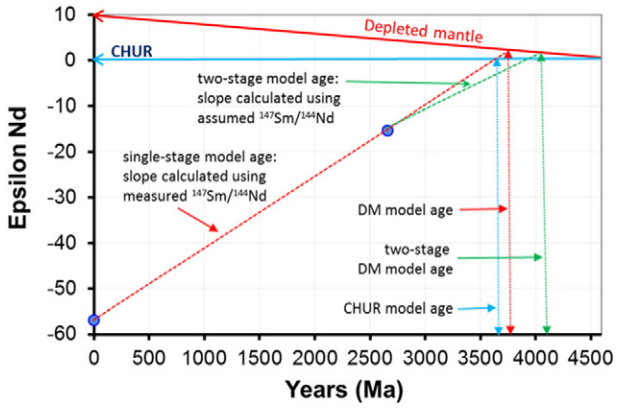

Fig. 3. Nd model ages. Single stage Nd model ages (T_{CHUR}, T_{DM}) assume no fractionation of Sm/Nd (=measured ratio). The intersection of the sample evolution curve with the mantle evolution curve (chondritic (CHUR) or depleted mantle (DM)), defines the model age. Two-stage model ages (T_{2DM}) assume a change in Sm/Nd at some point in the crustal history of the protolith. For felsic magmatic rocks this is typically the magmatic age. Prior to this (i.e., for ages older than the magmatic age) a model $^{147}Sm/^{144}Nd$ ratio is used, typically that of average continental crust. As for calculating ε_{Nd}, values of $^{147}Sm/^{144}Nd$ and $^{143}Nd/^{144}Nd$ have to be assigned for the DM and CHUR reservoirs. DM values used here are 0.2136 and 0.513163.

(Fig. 3) assume that the dominant fractionation (i.e., change) of Sm/Nd occurred as a result of the mantle extraction event, i.e., crustal processes have not significantly modified this ratio. Although mostly not realistic (as shown by the changes in average Sm/Nd in crustal reservoirs; Table 2), it is evident that they can provide useful results (e.g., Bennett and DePaolo, 1987). One consideration with single stage models is that model ages are increasingly unreliable with increasing Sm/Nd ratios (as sample evolution curves become more sub-parallel with mantle evolution curves) and such model ages should not be calculated for $^{147}Sm/^{144}Nd$ ratios over 1.4–1.5. Most felsic igneous rocks have $^{147}Sm/^{144}Nd$ ratios between 0.09 and 0.12 (e.g., Sun et al., 1995).

Two-stage model ages (T_{2DM}) are increasingly being used for felsic igneous rocks in particular (e.g., Liew and McCulloch, 1985) to correct for changes in Sm/Nd ratios, produced by processes such as partial melting, fractional crystallisation, magma mixing, alteration, etc. Such models are typically calculated using the measured $^{147}Sm/^{144}Nd$ ratio back to the magmatic age of the rock and an assumed (not the measured) $^{147}Sm/^{144}Nd$ ratio for calculating the sample evolution curve prior to the crystallisation age (see Fig. 3). In this work an assumed $^{147}Sm/^{144}Nd$ ratio of 0.11 has been used, equivalent to the average upper continental crust value using Sm and Nd values from Rudnick and Gao (2004). Liew and McCulloch (1985), for example, used a value of 0.12. Two stage depleted mantle model ages may be younger or older than single stage ages, depending on the measured and assumed $^{147}Sm/^{144}Nd$ ratios used. Empirical evidence suggests two stage model ages give more consistent model ages on a regional basis (Champion and Cassidy, 2008; Champion, 2013). They also allow model ages to be calculated for samples with high measured $^{147}Sm/^{144}Nd$ ratios. Model age calculations with a similar interpretation are widely used for the Lu–Hf system, especially for in-situ measurements on minerals such as zircon, e.g., Griffin et al. (2004); Murgulov et al. (2007). Notably, the methodology for two stage Nd depleted mantle model ages is essentially identical to the approach used for calculating hafnium (Hf) model ages from Hf in zircon analysis, where Lu/Hf ratios of the parent magma are assumed (e.g., Kemp et al., 2009).

Because of the complexities of Pb, U and Th fractionation during global- to province-scale geochemical processes, modelling of isotope systematics is more complex and commonly empirical for this system. Isotopic models of Pb growth have been developed both at global (e.g., Stacey and Kramer, 1975; Cumming and Richards, 1975) and province (Carr et al., 1995; Sun et al., 1996; Thorpe, 1999) scales. Although the global models provide ages that are generally valid, more accurate model ages are provided by province models. In addition to predicting the age of many deposits to within 10 million years of ages determined by independent methods, such as zircon U-Pb, the Abitibi-Wawa and other provincial Pb models provide information about lead source reservoirs, and in detail model Pb evolution more accurately. Many of these provincial or local models are in fact mixing models between separate growth curves—commonly, but not exclusively, more evolved and more juvenile growth curves. In some cases (e.g., the Lachlan model of Carr et al., 1995) the two end-member curves are isotopically distinct, whereas in other cases the end-member curves share common features such as $^{206}Pb/^{204}Pb$, $^{207}Pb/^{204}Pb$ and $^{208}Pb/^{204}Pb$ at the start of the modelled growth, with the changes in trajectory defined by the $^{238}U/^{204}Pb$ (μ) ratio or other parameters (e.g., Thorpe, 1999). Accordingly, the utility of isotopic mapping with Pb isotopes comes in measuring the mixing of Pb sources, either directly using μ (Huston et al., 2014) or indirectly by estimating mixing ratios of the modelled end-member sources (Huston et al., 2016-in this volume). Both methods can be used to produce isotopic maps and both are illustrated later in this contribution.

Like Sm–Nd, Pb isotopic ratios (e.g., $^{206}Pb/^{204}Pb$ or $^{207}Pb/^{204}Pb$) should only be used if sample ages are similar, e.g., for Pb from galena, mineral deposits should be of generally similar ages. Huston et al. (2014) discussed variations in both $^{207}Pb/^{204}Pb$ and μ, but preferred

the latter as it provides better comparisons for deposits of different ages (as the growth of radiogenic lead is accounted for). Like Nd model ages, therefore, regional isotopic maps based on Pb μ values can be used to map respective source reservoirs. For lead in VHMS deposits, for example, this is generally providing information about the upper crust (in contrast to neodymium in felsic magmatic rocks which is largely providing information about the lower crust and/or upper mantle). Like variations in Nd model ages, variations in μ can be described as "juvenile" and "evolved" in reference to isotopic sources. For Pb, juvenile refers to a source that was extracted from the mantle close to the time of mineralisation, and evolved refers to a source (or component) that has a time-integrated crustal signature, that is the source was most likely resident in the crust for a significant period of time prior to isotope extraction. For lead, a juvenile source is less radiogenic, with a low μ, whereas an evolved source is more radiogenic, with high μ. Our experience in Pb isotope mapping is that because Pb isotope growth models are provincial, so too is isotopic mapping, i.e., such Pb maps are best used at geological province scale. A number of authors (e.g., Doe and Zartman, 1979; Zartman and Doe, 1981) have attempted to develop global Pb growth models in a tectonic context.

3.1.1. Residence ages

Residence ages (T_{Res}) which simply equal the model age (for the Sm–Nd system usually the Nd depleted-mantle model age) minus the crystallisation age, can also be used as a variable in isotopic maps.

$$T_{Res} = T_{2DM} - T_{magmatic} \quad (6)$$

For the Sm–Nd system and granites, such ages provide an indication of the relative age of the protolith of the granite in question, i.e., the time between when specific crust was created and its reworking to produce the granite. Granite formed by the reworking of largely juvenile crust will have young residence ages, whilst those forming in older crust will have old residence ages. The combination of model and residence ages (T_{2DM}, T_{Res}) with geochronological data (magmatic and xenocrystic ages) is particularly powerful in that it not only provides an indication of the age of the crust in a region and when that crust was reworked, but provides additional constraints on the protolith and components within individual granite units. This approach has been used to great effect in zircon studies where U–Pb ages and Lu–Hf isotopic data can be collected for individual grains or subgrains (e.g., Belousova et al., 2010).

3.1.2. Model assumptions

It should be noted that model (and residence) ages (and other model-based isotopic variables) are just that—a model. As outlined by many workers (e.g., DePaolo, 1988; Kemp et al., 2009) the origin of the isotopic signature of a rock can be complex. Model age calculations contain a number of assumptions:

- source characteristics are known and correct, i.e., for Nd the modelled mantle is correct; for Pb, the evolution model used is correct
- for Sm–Nd, the growth of the crust represents one event
- for Sm–Nd, the various magmatic components are understood. For model ages calculated from granites this typically reduces to assuming a uniform infracrustal protolith (an assumption that may often not be valid)
- for Sm–Nd, the behaviour of Sm/Nd in crustal growth processes, and subsequent reworking, are understood and approximate the Sm/Nd ratios used in the model
- for Pb, the ratios used in the model calculation do not contain radiogenic Pb produced after Pb deposition
- the isotopic systems have remained closed
- isotopic systems have not been effected by post-emplacement/post-depositional processes, including the incorporation of exogenous isotopes.

These assumptions, and their interpretation, will vary with the rock type being investigated. For felsic igneous rocks (for which Nd model ages are commonly used) calculated model ages, if taken at face value, imply that the crustal protolith for the sample in question was largely homogeneous (one source component) and essentially formed in a single event. Neither of these assumptions will be universally and probably only rarely, true, and even when these criteria are met the model age is still only an approximation, given the various uncertainties. There is abundant evidence that crustal protoliths can be complex (as readily evidenced by the geological record in many regions), as well as much literature on the demonstrated role of crustal, juvenile and assimilated components in felsic magmatism (e.g., Kemp et al., 2007, 2009). With regards to complex crustal protoliths, the calculated Nd model ages are best thought of as average ages. The situation can be clarified to some extent by the use of complementary data, such as magmatic ages, inherited zircon ages, other isotopic systems, especially in-situ analysis of magmatic and xenocrystic minerals (e.g., Lu–Hf and oxygen isotope analysis of zircons), as well as use of geological ages from regional geology (e.g., Bennett and DePaolo, 1987; Liew and McCulloch, 1985). The variability in Nd model ages in regions where multiple samples exist can also be used to help constrain and interpret regional Nd model age data (e.g., Champion and Cassidy, 2008).

As for Nd, the Pb isotope ratios and derived parameters represent averages for the sources sampled. However, as long as the Pb was not added or removed subsequent to mineralisation or crystallisation, the ratios and derived parameters reflect those of the (average/mixed) source reservoir. The reliability of Pb isotope model ages can be tested by comparing with ages obtained by other, more robust, methods.

4. Interpreting isotopic signatures: In space and time

One important way to help decipher the (geological and) isotopic data for magmatic rocks and mineral deposits is by looking at both geographic and secular changes of isotopic signatures, i.e., changes in isotopic signatures and model ages (or other variables, such as μ for the Pb system; Table 1) through space and time (e.g., Zartman, 1974; Bennett and DePaolo, 1987; Wooden et al., 1998; Huston et al., 2014; Champion, 2013; Mole et al., 2013, 2014). Time can be incorporated either via a series of time slices (e.g., Mole et al., 2014), and/or by use of time-independent (or largely time-independent) isotopic variables (such as model ages for Sm–Nd, Lu–Hf, Re–Os, or μ values for U–Th–Pb). Displaying and interpreting geographic variation in isotopic data relies on some method of data classification. In areas with small data sets and/or simply-behaved data, data classification may rely on 'simple', somewhat subjective, contouring (e.g., Zartman, 1974; Huston et al., 2014; Fig. 4). This approach can also be extended to more complex data sets, Wooden et al. (1998), for example, utilised a slightly different approach, breaking their Pb isotopic data into a number of classes and showing these spatially on a number of figures, for both $^{206}Pb/^{204}Pb$ and $^{208}Pb/^{204}Pb$.

The simplest way to rapidly (and more objectively) visualise regional isotopic data, such as Nd model ages, is by computer-assisted visualisation, such as interpolated images, where data values are grouped and displayed as classes, such as that shown in Fig. 5. This figure highlights a number of points. Firstly it is evident that regional changes in isotopic signature, i.e., in Nd model ages, are readily recognisable, and inferences from the figure correspond well to what can be deduced from the isotope data alone (Fig. 6), i.e., the image provides constraints on crustal growth that may have occurred in the Pilbara region. The interpolation also has a number of advantages and disadvantages: actual interpolation will depend to some extent on the interpolation process used and the technique used to identify intervals (colour bins)—both of which will affect the produced image. There is a large field of literature on this which is beyond the scope of this paper (e.g., see Slocum et al., 2009, and references therein).

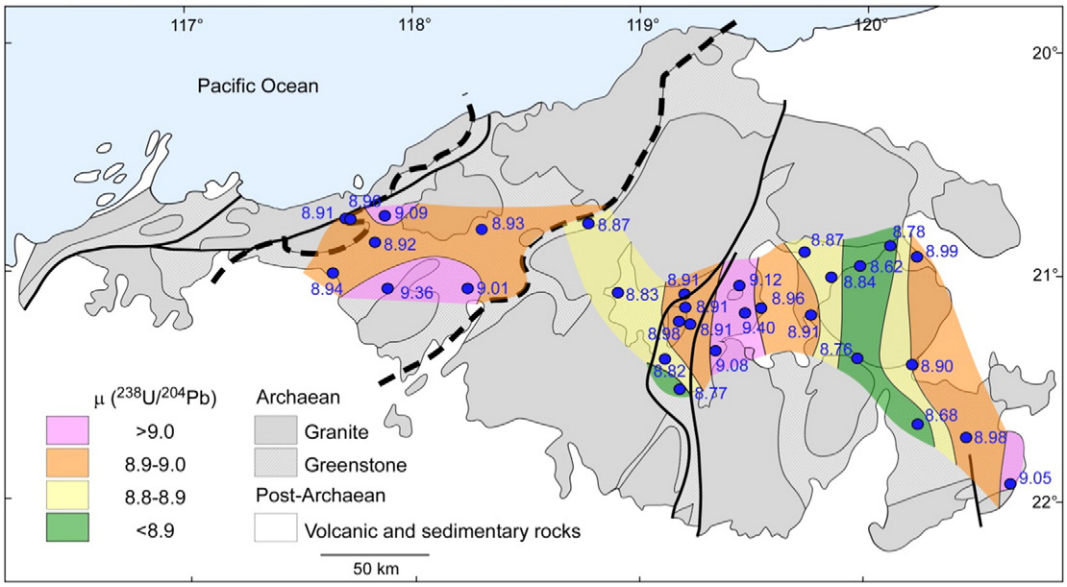

Fig. 4. Preliminary μ ($^{238}U/^{204}Pb$) isotope map for the Pilbara Craton. Isotopic data based on galena and other Pb-rich material from Archean mineral deposits. Data and data sources given in Huston et al. (2002).

The approach used here follows that of Champion (2013) who found that natural neighbour classification using natural breaks in data values (as against equal intervals or equal counts) worked well. Gridding performed in ArcMap™ was undertaken using Natural Neighbour Interpolation with intervals based on Natural Breaks (Jenks), i.e., intervals were determined by the software (the reason for the non-linear intervals in the resultant images, e.g., Fig. 5). The natural breaks techniques used by that software follows the Jenks optimisation method—also known as the goodness of variance fit—which identifies thresholds (identified intervals) which optimise (i.e., minimise) the sum of squared deviations of interval means. Slocum et al. (2009) have discussed the relative merits of different data classification procedures.

The general approach outlined above is applicable to most radiogenic isotopic systems, e.g., Sm–Nd, Lu–Hf, U–Pb, Re–Os and variables calculated from such data, e.g., μ values, Hf model ages, Os model ages (Table 1). Such images are particularly useful at regional to continental scales (e.g., Zartman, 1974; Farmer and DePaolo, 1983, 1984; Bennett and DePaolo, 1987), and it is clear that these images have a variety of uses, including metallogenic studies (e.g., Wooden et al., 1998; Huston et al., 2014). The vast amounts of isotopic (and other) data now available and being produced at an ever increasing rate, means that construction of such isotopic maps will become both easier and more detailed. Champion (2013), for example, recently produced an Nd model age map for the whole Australian continent, and documented a wide variety of regional geographic changes in isotopic signatures and how they relate to crustal growth, continental assembly and metallogeny. A range of regional Nd and Pb isotopic maps for various Archean cratons around the world, and parts of Australia, were highlighted in Huston et al. (2014, 2016-in this volume). Those authors used Pb signatures from sulphide minerals to generate regional maps based on μ values (Yilgarn Craton) and mixing meaurements (New South Wales, extending the pioneering work of Carr et al., 1995), which have proved useful in identifying both juvenile crustal terranes and for mapping the extent of such terranes, and related metallogeny. Other examples of Pb provinces are discussed in Tosdal et al. (1999), and include the Pb isotope provinces of the western United States (e.g., Zartman, 1974; Wooden et al., 1998) based on Pb signatures of granites, other rocks, and sulphide minerals, and that in the central Andes of South America (e.g., Macfarlane et al., 1990; Kamenov et al., 2002), based on Pb signatures of sulphide minerals.

The visualisation approach, as used by Champion (2013) recognises that absolute values of isotopic variables such as model ages, μ values, are much less important (or significant) than geographical and/or secular changes in such variables (an implicit recognition of the assumptions behind the calculations of such variables). The identification of such geographical and/or secular changes is particularly informative in regions with multiple episodes of magmatism and mineralisation, e.g., the Pilbara (Huston et al., 2002; van Kranendonk et al., 2007). A simple example to illustrate how to interpret such isotopic maps, as well as the relative advantages and disadvantages of such images, can be illustrated by looking at firstly Sm–Nd and then U–Th–Pb isotopic data and images from the Archean Pilbara Craton, Western Australia (Figs. 6, 5, and 4).

In the East Pilbara Terrane (EPT; terminology follows Van Kranendonk et al., 2007) it is clearly evident that ca. 2.93–2.85 Ga and older felsic magmatism is reworking older (ca. 3.6–3.5 Ga Pilbara crust; Fig. 6). These rocks show generally similar T_{2DM} but increasingly negative ε_{Nd} through time, both features consistent with crustal reworking (e.g., Champion, 2013). The figure shows an obvious broad zonation in model ages for ca. 2.93–2.85 Ga granites, however, across the craton with a significant jump in model ages and ε_{Nd} (and T_{Res}) values across a zone that approximates the boundary between the East Pilbara Terrane and the West Pilbara Superterrane (WPS). Consideration of T_{2DM} and ε_{Nd} data across this zone shows that both markedly decrease from east to west (Fig. 6).

The simplest, though not the only, interpretation is that the basement to the WPS is geologically younger than that which underlies most of the EPT. Van Kranendonk et al. (2007) interpreted the EPT as a cratonic nucleus upon which components of the WPS were added or grew. It is notable that there is not a one-to-one relationship between the isotopic break and the EPT-WPS boundary. Younger model ages in the EPT are confined to younger magmatism (ca. 2.95–2.85 Ga) in the western part of the EPT, which were attributed by Champion and Smithies (2000) to WPS geological events affecting that part of the EPT. There is additional support for this in the belt of unusual high-Mg dioritic magmatism that runs along and outboard of the western margin of the EPT (e.g., Smithies and Champion, 2000). Fig. 6 also highlights the primitive isotopic signature of the rocks in the western part of the Sholl Terrane of the WPS, which Smithies et al. (2005) have interpreted as a juvenile arc.

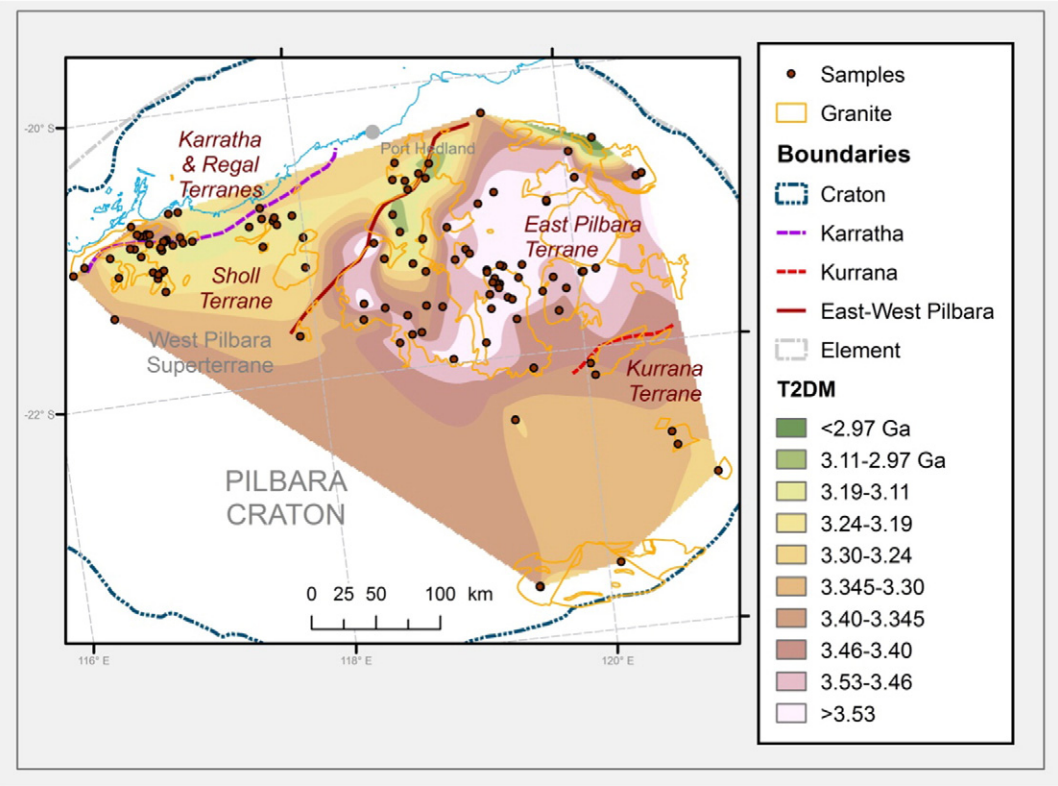

Fig. 5. Gridded Nd two-stage depleted mantle model age (T_{2DM}) map for the Pilbara Craton, Western Australia. Isotopic data used to create the grid are also shown (Data and data sources are in Champion, 2013). Also shown are: the boundary between the Karratha and Regal terranes and the Sholl Terrane (all three comprise the West Pilbara Superterrane); the boundary between the West Pilbara Superterrane and East Pilbara Terrane and the boundary between the East Pilbara Terrane and the Kurrana Terrane (nomenclature follows van Kranendonk et al., 2007). Grid colours in areas with no samples are purely based on interpolation and may have no relationship with underlying deeper crust.

It should be noted that there are other possible interpretations for the change in isotopic signature across the East Pilbara Terrane/West Pilbara Superterrane boundary. For example, the change may simply reflect much greater juvenile input in the West Pilbara Superterrane at or prior to ca. 2.95–2.85 Ga. In this scenario this is no requirement for a change in basement across this margin, but rather a significant change in the proportion of juvenile versus East Pilbara-style crust. This is a consistent difficulty when interpreting regional changes in Nd model ages and other isotopic data. It shows that, like much geological data, there are a variety of ways to interpret isotopic data such as Nd model ages, and other supporting geological and geophysical evidence should always be included where possible. For the Pilbara example, the consistent lack of older model ages in the west, and the geological evidence for continental margin-style magmatism (e.g., Smithies et al., 2005) support the terrane boundary theory. Regardless, the isotopic data are recording a difference that may be significant in regards to potential mineral systems and metallogeny (e.g., Huston et al., 2014; see below).

The Pilbara example shows that, although there are a variety of evident secular changes, there are three general end-members that can be defined on the behaviour of model ages, ε_{Nd}, (and other derived isotopic parameters) through time and/or space (see Table 3). As shown by Champion (2013) for the Australia-wide compilation, various combinations of these three end-member trends are evident in all regions of Australia. Perhaps the most distinctive and most straight forward to interpret is the case for constant model ages (Type 1 in Table 3), though such scenarios are also probably the most uncommon. Many early workers documented such patterns, e.g., Bennett and DePaolo (1987) and interpreted them to demonstrate crustal reworking, with minimal involvement of juvenile material.

Another feature illustrated by the Pilbara example, is that users need to be cautious both of regions with no or limited data and of the artefacts of interpolation. Also it is evident that the interpolation process itself tends to smooth data somewhat, i.e., simplify the regional isotopic variation (obviously scale dependent; e.g., compare the range of model ages for the EPT in Fig. 6 versus the resultant image in Fig. 5). This has both advantages, i.e., makes interpretation easier, but also disadvantages (in that complexity can be lost from regions), e.g., subtle changes in isotopic signature through time, such as that documented by Kemp et al. (2009) for granites in southeastern Australia, will not be obvious within the gridded data. Such interpolated figures should always be used in conjunction with the original isotopic data, i.e., with ε_{Nd}-time and T_{2DM}-time plots (as in Fig. 6), to fully explore the variations of isotopic signatures and complexities within each crustal block. It is also advisable to use other data (geological and geophysical). This includes data from additional isotopic systems and resultant images.

A preliminary regional μ ($^{238}U/^{204}Pb$) map compiled from galena from Archean mineral deposits is also available for the Pilbara region (D. Huston, unpublished; Fig. 4). Unlike the examples discussed below and elsewhere (e.g., Huston et al., 2016-in this volume), the Nd and Pb isotope maps for the Pilbara region have more differences than similarities. Most notably, the Pb isotope data appears to be picking up a conspicuous zoning in the central EPT not evident in the more uniform Nd model ages in that region. These differences, although not fully understood, must be partly a reflection of the disparate reservoirs each isotope system is informing on, namely felsic magmatism largely derived from the middle and lower crust (±mantle) for Sm–Nd, and basalt-dominated greenstone sequences, largely derived from the mantle (±crust) for Pb (e.g., van Kranendonk et al., 2007; Champion and Smithies, 2007). There are some similarities also, e.g., both the Nd and Pb images are picking up the more juvenile zone in the western part of the EPT and the East Pilbara Terrane/West Pilbara Superterrane boundary (although data for Pb is limited in these regions and should be interpreted with caution).

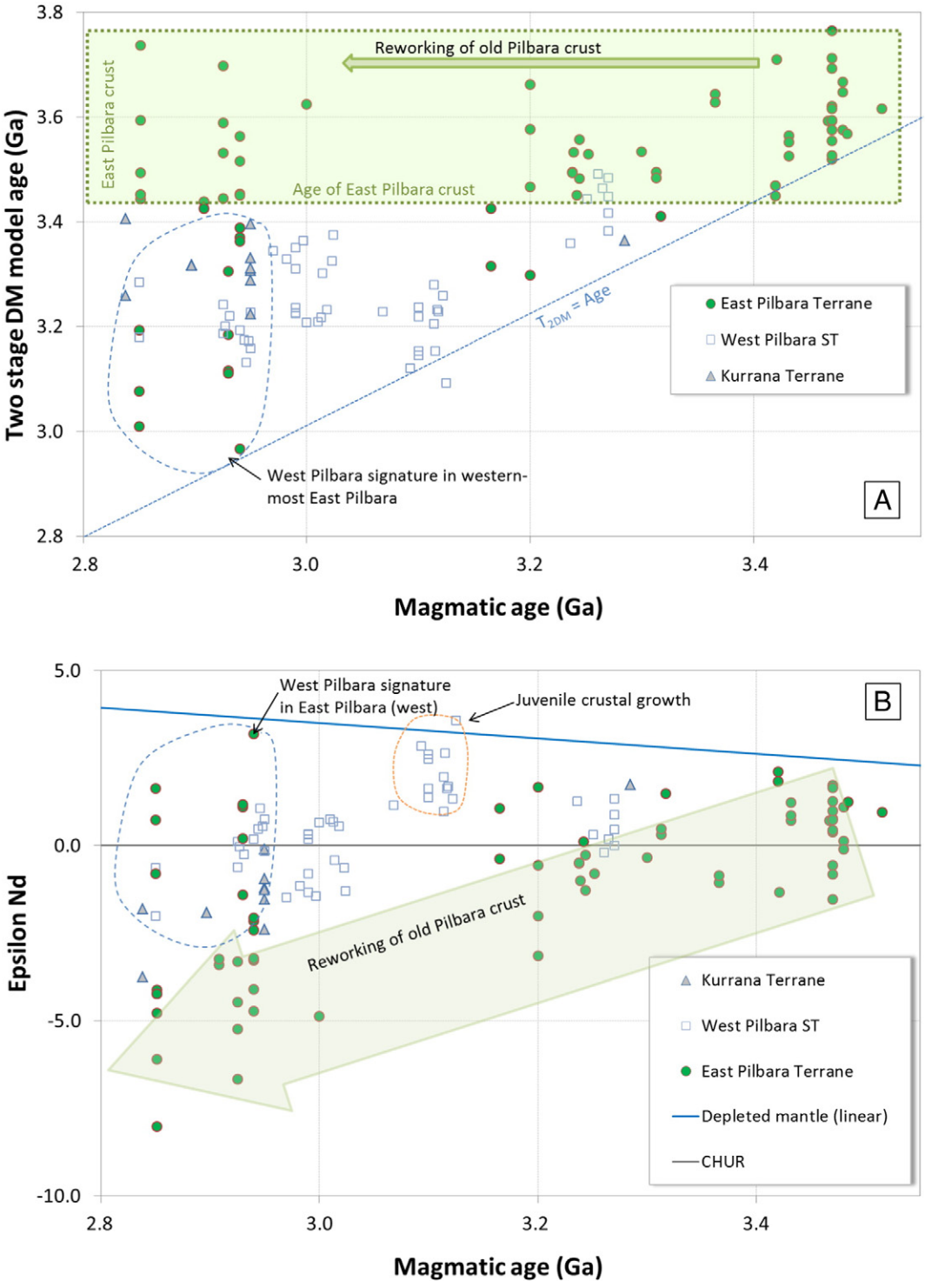

Fig. 6. Two-stage depleted mantle model ages (A) and ε_{Nd} (B) versus magmatic ages for the Pilbara Craton, Western Australia. The East Pilbara Terrane largely shows decreasing ε_{Nd} and approximately constant T_{2DM} with decreasing magmatic age (Type 1 behaviour Table 3), consistent with reworking of old crust with minimal juvenile involvement. The exceptions to this are 2.95–2.85 Ga magmatism in the western part of the East Pilbara Terrane which include a more significant juvenile component (younger T_{2DM}, more positive ε_{Nd}), probably related to growth of the West Pilbara Superterrane (e.g., Champion and Smithies, 2000). Data are shown spatially in Fig. 5. Refer to Champion (2013) for data sources.

As will be discussed below, most current metallogenic interpretations using combined isotopic systems have concentrated on similarities between the systems (e.g., Huston et al., 2014). The latter authors, for example, produced a Pb isotopic map for the Eastern Goldfields Superterrane of the Yilgarn Craton that is in close agreement to the Nd isotopic map for the same region and based on this co-incidence of isotopic signals, developed models for VHMS mineralisation in that, and other, Archean regions. These two systems have been complemented by Mole et al. (2014) who recently produced a series of time-stamped regional Hf model age maps for various regions in the Yilgarn Craton, exploring the relationship between the crust and nickel mineralisation through time, building on previous interpretations based on the Nd data (e.g., Cassidy

Table 3
Secular variations in T_{2DM} and ε_{Nd} in felsic magmatism and possible interpretations. Note that a range of isotopic signatures (e.g., ε_{Nd} and T_{2DM}) are indicators for multiple age sources and/or components.

Type	Variations with decreasing age	Interpretation	Examples
1	T_{2DM} approximately constant (especially maximum values) ε_{Nd} decreasing	Largely reworking of pre-existing crust. Any juvenile input is cryptic.	South-western United States (Bennett and DePaolo, 1987); East Pilbara Terrane, Western Australia (Champion, 2013)
2	T_{2DM} decreasing ε_{Nd} ~ constant	Involvement of both pre-existing crust and juvenile material (either reworking of young crust and/or direct mantle input).	Pine Creek-Tennant Creek-Tanami-Aileron provinces, Northern Territory (Champion, 2013)
3	T_{2DM} decreasing (markedly) ε_{Nd} increasing (to constant)	Significant juvenile input (often related to long-lived accretionary orogens). Pre-existing older crust thinned or largely absent. May be associated with a significant sedimentary component.	Tasman Orogen (e.g., Kemp et al., 2007); western United States (Farmer and DePaolo, 1983)

et al., 2005; Begg et al., 2010). This makes the Yilgarn Craton one of the better, perhaps the best, isotopically studied strongly mineralised region on earth. Certainly the combined use of different isotopic systems allows even more detailed investigation of the possible relationships between crustal blocks and metallogeny, and also allows a better understanding of the possible processes that may be controlling such metallogeny (e.g., Cassidy et al., 2005; Begg et al., 2010; Huston et al., 2014; Mole et al., 2012, 2013, 2014). The Yilgarn example and a number of other examples of using regional isotopic maps—with either just Nd model age maps or the latter in combination with other isotopic maps (Pb, Lu–Hf)—are discussed below with regards to metallogenic implications and interpretations.

5. Radiogenic isotope maps and mineral systems

Radiogenic isotopes in mineral systems can be used in a variety of ways at a variety of scales. In this review we concentrate on the larger-scale parts/processes of mineral systems, i.e., continent to craton and craton to regional scales (larger scales in Fig. 1), which may either be directly or indirectly identifiable in regional isotopic maps. These include the following:

- Demonstrable empirical relationships between mineral systems and isotopic domains, as documented for specific regions, e.g., the Yilgarn Craton (mesothermal Au, VHMS and komatiite-associated nickel deposits; Cassidy and Champion, 2004; Cassidy et al., 2005; Huston et al., 2005; Mole et al., 2014), on the regional scale, e.g., western United States (porphyry Cu and Mo; Zartman, 1974), or on the continental scale, e.g., Proterozoic IOCG belts in Australia (Skirrow, 2013). Such empirical observations can be extracted, tested and applied as predictive tools. One good example of the latter is the relationship between isotopically primitive (juvenile) terranes and fertility of VHMS deposits, which based on initial observations in the Yilgarn Craton (Cassidy and Champion, 2004; Cassidy et al., 2005; Huston et al., 2005), were tested and shown to be applicable for Archean and Proterozoic VHMS deposits (Huston et al., 2014).
- Identification of old, especially Archean, cratonic blocks, which may be metallogenically-endowed, but which may also have other favourable characteristics, e.g., regions of thicker lithosphere which focus mantle melts around their margins (e.g., Begg et al., 2010; Mole et al., 2014). Old crustal blocks and their mantle lithosphere may also have been the (repeated) focus of important mantle melts, providing potential metal sources for later reworking (e.g., Groves et al., 2010, though see Arndt, 2013 for an alternative view).
- Identification of old continental margins, especially those consistent with an accretionary setting. Such settings are favourable sites of contemporaneous mineralisation, e.g., porphyry deposits, especially where accompanied by juvenile isotopic signatures (Champion, 2013). This also includes the ability to identify and map continental fragments within such accretionary orogens, e.g., interpreted island arc fragment in northern Queensland (see section 5.5). These blocks may themselves be metallogenically important. Accretionary orogens are also potential sites for metasomatism of the lithosphere, again providing potential metal sources for later reworking (e.g., Groves et al., 2010).
- Identification of juvenile zones, either marginal or internal, which may indicate extension and possible rifting and associated mineralisation, such as epithermal, VHMS (e.g., Huston et al., 2014, 2016-in this volume), or primitive arc crust and associated mineralisation, e.g., porphyry Cu–Au.
- Identification of crustal breaks, which may represent major faults and sutures, and may have acted as fluid pathways for fluids and magmas (e.g., Wooden et al., 1998). They can also serve to delineate natural boundaries for metallogenic terranes or transitional boundaries which may be important (e.g., VHMS deposits, Huston et al., 2014; porphyry deposits, Zartman, 1974).

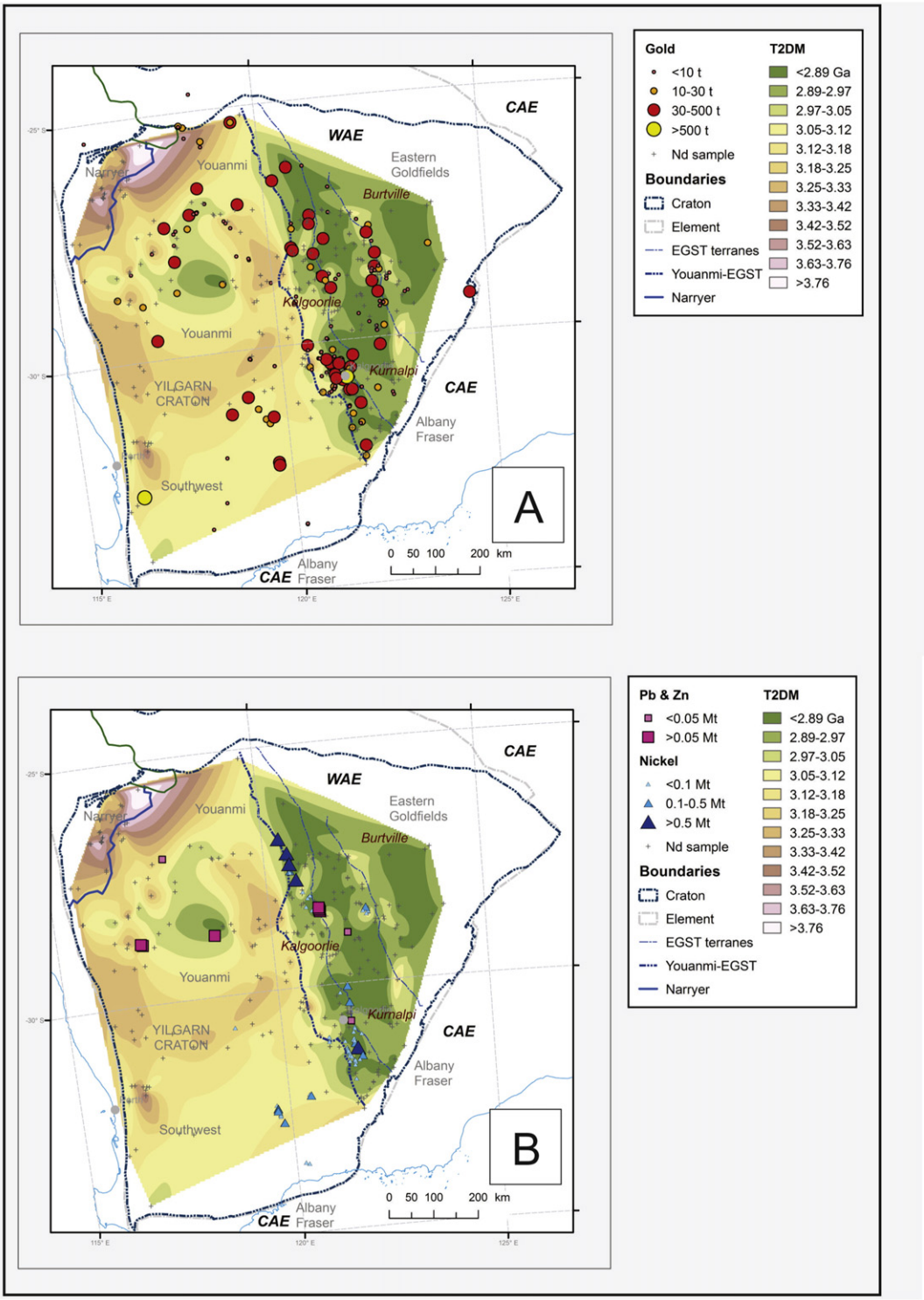

Fig. 7. (A) Location of gold and (B) nickel (nickel sulphide) and volcanic hosted massive sulphide (Pb–Zn) deposits, by size, in the Yilgarn Craton, superimposed over gridded two-stage depleted mantle model age (T_{2DM}) map. Image constructed from 305 data points. Data and data sources listed in Champion (2013). Grid colours in areas with no samples are purely based on interpolation and may have no relationship to the underlying crust. Mineral deposit locations are from the Australian Mines Atlas (http://www.australianminesatlas.gov.au/). Yilgarn Craton terrane boundaries from Cassidy et al. (2006). WAE = Western Australian Element, CAE = Central Australian Element. Element boundaries as in Huston et al. (2012).

- Baseline maps which help to identify regions/periods characterised by greater (or lesser) magmatic, especially mantle input, e.g., the western boundary of the East Pilbara terrane (Fig. 5) which has been overprinted by younger crustal growth or, possibly the region around the giant Olympic Dam IOCG deposit (see below).

Many of the above appear to act in combination with one another and also act repeatedly; examples of each are discussed below. These examples also highlight some of the steps in going from conceptual mineral systems to exploration targeting, e.g., as discussed by McCuaig et al. (2010).

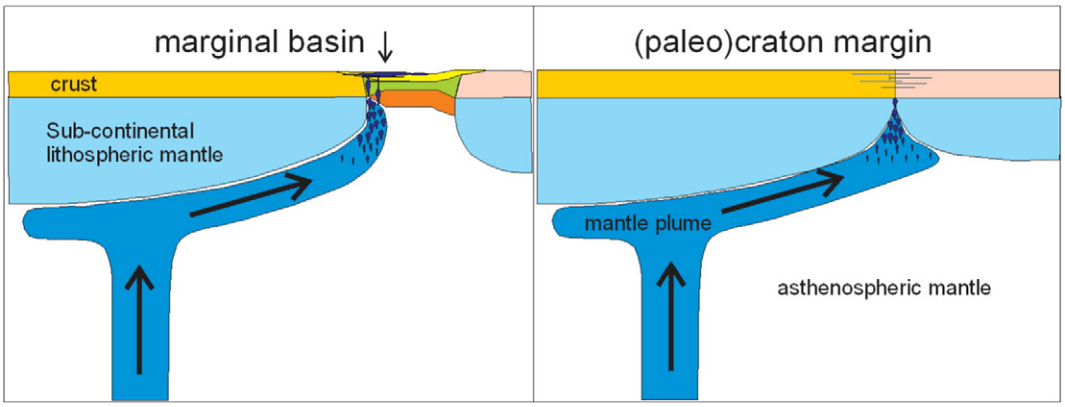

Fig. 8. The generalised Begg et al. (2010) model illustrating preferential flow of impinging mantle plume towards, and subsequent localisation of nickel sulphide deposits within, thinner lithosphere along the margins of thick (>150 km) lithospheric blocks, e.g., with intervening marginal basin (A) or along an old paleo-margin (B). Either model may be applicable for the Yilgarn Craton (Fig. 9). Figure modified from Begg et al. (2010).

5.1. Regional isotopic signatures in the Yilgarn Craton and Ni, Cu-Pb–Zn and Au deposits

The impetus behind the Nd model age map of Australia (Champion, 2013) was the recognition of the apparent correlation between the regional Sm–Nd signature of granites of the Yilgarn Craton (Cassidy et al., 2002; Champion and Cassidy, 2007, 2008) and a range of mineralisation styles. Cassidy et al. (2005) and Huston et al. (2005, 2014) documented an apparent spatial association of larger komatiite-associated Ni (KANS), volcanic-hosted massive sulphide base-metal (VHMS) and orogenic Au deposits with crustal regions with specific isotopic signatures (Fig. 7). Komatiite-associated Ni–Cu deposits, for example, appear to be spatially associated with terranes with pre-existing evolved crust (Youanmi, Kalgoorlie, the 'older' eastern half of the Kurnalpi Terrane), as identified by isotopic signature, in this case Nd T_{2DM} model ages (Fig. 7). It was found that juvenile terranes are the least prospective for this mineralisation style. This relationship appears to hold even though both komatiite type and ages are variable. Cassidy and Champion (2004) and Cassidy et al. (2005) also recorded an apparent relationship between orogenic gold mineralisation and older crustal terranes (similar to that observed for KANS). Conversely, it has long been recognised there is an apparent antithetic relationship between komatiite-associated Ni and VHMS base-metal mineralisation (Groves and Batt, 1984), and Cassidy et al. (2005) and Huston et al. (2005) showed that the latter mineralisation in the Yilgarn is associated with terranes with isotopically primitive crust (and also HFSE-enriched, bimodal volcanic-plutonic associations and rift settings). These occur in the western part of the Kurnalpi Terrane, eastern parts of the Kalgoorlie Terrane, and the central 'younger' zone in the Youanmi Terrane (Fig. 7). As noted earlier, another way of identifying isotopically primitive or juvenile isotopic domains is via plots of residence ages (T_{Res}) derived from Nd data. These give residence times independent of age, and are ideal for identifying young (juvenile) versus older crustal domains. However, for regions such as the Yilgarn Craton where felsic magmatic ages are essentially similar (mostly 2680 ± 50 Ma), T_{Res} maps are essentially identical to T_{2DM} maps. Either works well and T_{Res} maps of the Yilgarn Craton also clearly identify the juvenile zones in both the Eastern Goldfields Superterrane (EGST) and the Youanmi Terrane and the spatial association of these with VHMS deposits.

The possible reasons for the isotopic-metallogeny correlations were not originally well understood, especially the link between both nickel and gold with regions of isotopically more evolved (i.e., older) crust, and Cassidy et al. (2005) speculated on a variety of reasons. This uncertainty, in part, reflected the not-surprising general correlation between the isotopic domains and identified geological terranes (Cassidy et al., 2006), e.g., the largest isotopic break across the craton coincides with the boundary between the Youanmi Terrane and the EGST. This correlation is not perfect, however. For example, although the juvenile isotopic zone in the EGST is broadly correlated with the western two-thirds of the Kurnalpi Terrane, it also crosses into the Kalgoorlie Terrane (in the north; Fig. 7). The broad primitive zone within the otherwise isotopically-evolved Youanmi Terrane is also another example. Overall, therefore, it was not clear whether the crustal isotopic signature, and its correlation with mineralisation styles, reflected a primary feature of the relevant mineral system or was simply a proxy for some other important feature. Subsequent work has demonstrated that it is probably both, with the VHMS deposits an example of the former and the KANS an example of the latter. These are discussed in more detail below.

The possible reasons for the correlation of moderately-evolved isotopic domains and gold endowment are more enigmatic and not well understood. Cassidy et al. (2005) suggested a combination of geological factors to explain the correlation, including the association of (older) plume magmatism, occurrence of subduction-modified mantle melts, as well as the presence of lithospheric-scale orogeny. Recent sulphur isotope data for the Yilgarn Craton (Xue et al., 2013) favours gold sourced from either crustal magmatic and/or mantle sources and appears to rule out leaching from komatiitic rocks and associated supracrustal sequences (though more data are required to confirm this). Of the likely magmatic candidates in the Yilgarn Craton only perhaps the more enriched (high-LILE) 'Mafic' group (Champion and Sheraton, 1997; Champion and Cassidy, 2007; Czarnota et al., 2010) has a spatial association with gold mineralisation. This association could also explain why the much more isotopically primitive Archean Abitibi Terrane in the Superior Province, Canada is also well endowed with gold. In the latter terrane there appears to be a close temporal association between gold mineralisation and similar enriched intermediate igneous rocks (Beakhouse, 2007). For the Yilgarn Craton, however, it has not been sufficiently demonstrated that such magmatism is indeed largely confined to specific isotopic domains or gold-endowed geological terranes and so the link between Au mineralisation and isotopic domains still remains unclear. Blewett et al. (2010); Czarnota et al. (2010) and McCuaig et al. (2010) suggested that the Nd model age map was mapping, by proxy, lithospheric architecture, i.e., identifying lithospheric-scale architecture adjacent to paleocraton margins. This is not dissimilar to models, such as those of Goldfarb and Santosh (2013), which suggested deep (possibly slab-related) fluids responsible for the Phanerozoic gold deposits of the Jiaodong Province in China, were channelled into the upper crust along continental-scale fault systems. Such faults occur proximal to old craton margins, readily identifiable by isotope systems such as Sm–Nd.

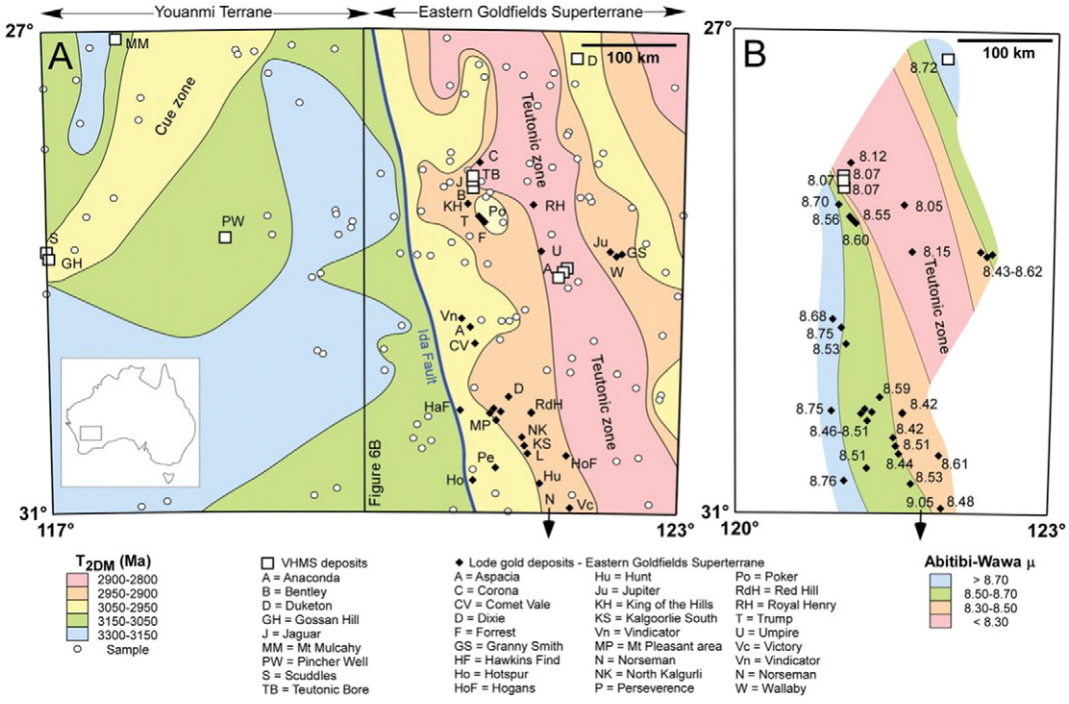

Fig. 9. (A) Variations in Nd model ages (T_{2DM}) of 2680 Ma to 2630 Ma granites and the location of selected mineral deposits in the Yilgarn craton (Champion and Sheraton, 1997; Champion, 2013), and (B) μ values calculated from galena lead isotope data from VHMS and lode gold deposits in the Eastern Goldfields Superterrane (data from Browning et al., 1987; McNaughton et al., 1990; Ojala et al., 1997; Salier, 2004; K. Cassidy, unpublished data; K. Czarnota, unpublished data). VHMS deposits indicated by open squares; lode gold deposits indicated by closed diamonds. The identities of major deposits and prospects are indicated by abbreviations keyed to the legend. Figure from Huston et al. (2014).

5.2. Isotopic domains and nickel mineralisation: Proxies for lithospheric architecture?

The relationship between nickel and crustal domains of the Yilgarn has been investigated by Barnes and Fiorentini (2010a, 2010b); Begg et al. (2010); McCuaig et al. (2010), in addition to Cassidy et al. (2005). Barnes and Fiorentini (2010a, 2010b, 2012) showed that most of the nickel endowment in the Yilgarn was concentrated within the Kalgoorlie Terrane and that that terrane was characterised by strongly olivine-enriched (cumulate) lithologies, relative to other terranes in the Eastern Goldfields Superterrane (although they also occur within the Youanmi Terrane). These authors suggested that the nickel endowment was a function of a number of factors that allowed high volumes and prolonged fluxes of komatiitic magmas into the Kalgoorlie Terrane crust, and they followed the craton-margin model of Begg et al. (2010); Fig. 8). The latter model suggests that lithospheric architecture was a major controlling factor in localising komatiitic melts with upwelling mantle plumes being preferentially channelled away from regions of thicker lithosphere to areas of thinner lithosphere, such as found on old craton margins, where they undergo decompression melting.

The Nd isotopic map of the Yilgarn Craton (Champion and Cassidy, 2007, 2008; Mole et al., 2013) supports this hypothesis with older (interpreted as thicker) lithosphere in the Youanmi terrane bound by younger (and thinner) lithosphere in the east, specifically the neighbouring Kalgoorlie Terrane. The Nd isotopic map is clearly identifying a major break between two lithospheric blocks that represents either an old continental margin (Begg et al., 2010) or perhaps a marginal basin (Krapez et al., 2000). Mole et al. (2014) expanded on this, utilising Lu–Hf from inherited zircons, in combination with their U–Pb ages, to show that similar lithospheric architecture controls may have operated for older komatiitic magmatism and associated mineralisation.

For the KANS mineral system, the crustal isotopic map is delineating lithospheric structure, i.e., acting as a proxy for lithospheric architecture, if indeed the model of Begg et al. (2010) is correct. Begg et al. (2010) have summarised a number of reasons why such lithospheric architecture, in particular thinner lithosphere along craton margins, may be more favourable for KANS and other ultramafic associated Ni–Cu–PGE mineralisation, including preferential flow of mantle plumes and melts to such regions, greater degrees of partial melting of the mantle in these regions, and greater access to the crust via large-scale fault systems. It is worth stressing the importance of scale. The isotopic systems are identifying favourable regions at a craton- to district-scale. It is evident that other controls on mineralisation exist at district- and camp-scales, such as the availability of sulphur, as shown by Fiorentini et al. (2012).

Nonetheless, it is evident that isotopic maps, such as the Nd model age map of the Yilgarn (Fig. 7), are very amenable to identifying old continental margins, and can, therefore, be used in exploration targeting as proxies for such pathways. It is clear, for example, from the Nd isotopic map of the Pilbara (Fig. 5) that old cratonic margins are readily identified (in line with the geological understanding of that region, e.g., Van Kranendonk et al., 2007). The identification of old margins is important for a number of other mineral systems. McCuaig et al. (2010) and Fiorentini et al. (2012) also highlighted a number of proxies, e.g., felsic volcanic rocks and VHMS mineralisation, for identifying extensional zones, which, like old continental margins, are another active pathway for komatiites.The identification of juvenile isotopic zones on Nd model age or Pb μ maps can also act as a proxy for the recognition of major rift zones and zones of extension. As discussed specifically in the example below, such zones are evident within the Yilgarn Craton, especially in the EGST, at a variety of scales. Notably, in the Yilgarn Craton, at least, KANS mineral systems appear to be more closely spatially associated with second order extensional zones, i.e., marginal to or bordering the main juvenile isotopic zone.

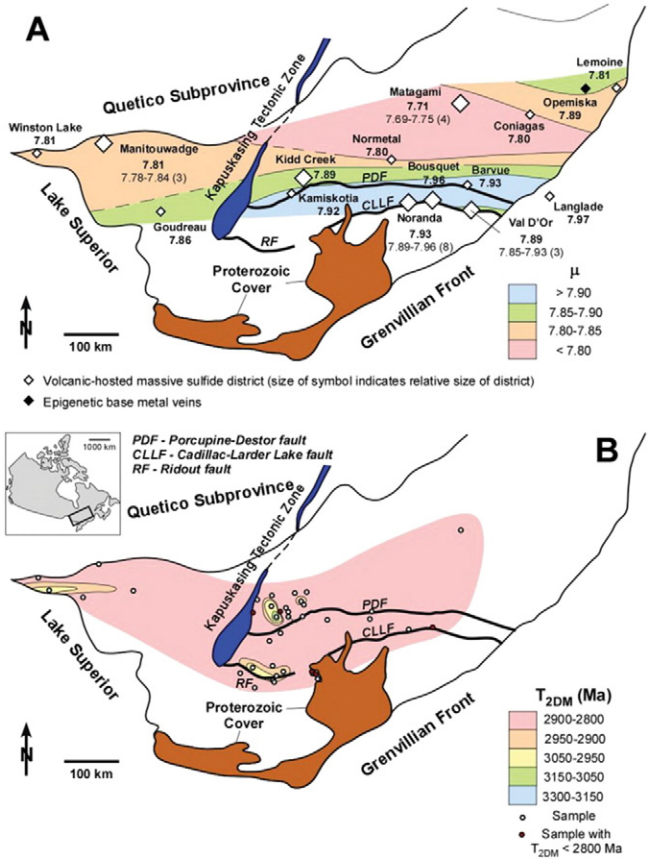

Fig. 10. (A) Variations in μ for VHMS deposits and (B) variations in T_{2DM} of ~2700 Ma felsic to intermediate volcanic and intrusive rocks from the Abitibi-Wawa subprovince. Values were calculated from least radiogenic Pb isotope galena analyses from Thorpe (1999), using the Abitibi-Wawa model, with number of deposits in districts in parentheses (except districts where data from only one deposit are available). Values for T_{2DM} were calculated using whole-rock Nd–Sm isotope data from Barrie and Shirey (1991), Vervoot et al. (1994), Prior et al. (1999), Ayer et al. (2002), Polat and Kerrich (2002), Mercier-Langevin et al. (2007), and Ketchum et al. (2008). Figure from Huston et al. (2014).

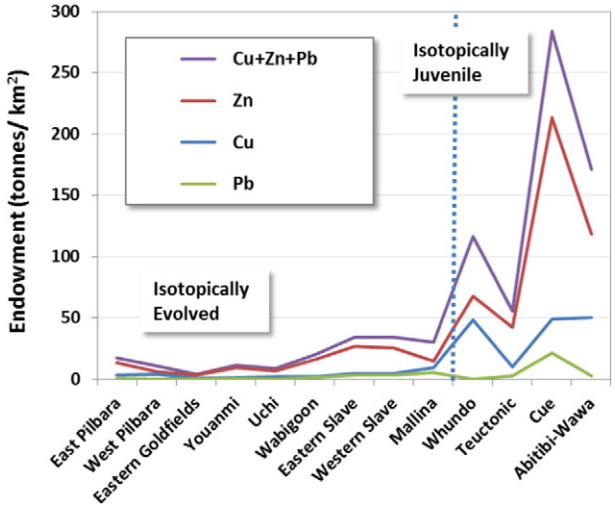

Fig. 11. Plot of Cu, Zn, Pb and combined CU–Pb–Zn (volcanic-hosted massive sulphide) metal endowment (in tonnes per km^2) for Archean cratonic blocks in Canada and Australia, highlighting the much greater endowment in isotopically primitive blocks. Endowment figures taken from Table 3 of Huston et al. (2014), which were based on Franklin et al. (2005) updated to include new data from company press releases.

5.3. Isotopic domains and VHMS mineralisation: From empirical to predictive

Huston et al. (2005, 2014) investigated the relationship between Nd isotopic domains and VHMS mineralisation for the Yilgarn Craton (Fig. 9). Importantly, they were able to show that there was a reasonable empirical relationship between the location of known VHMS deposits and more juvenile crust, i.e., younger T_{2DM} zones on the Yilgarn T_{2DM} map (Fig. 9). Huston et al. (2014) also produced Pb isotope maps based on μ values ($^{238}U/^{204}Pb$) calculated using Pb isotope signatures of galena and other Pb-rich minerals from a variety of Archean mineral deposits including VHMS and orogenic gold deposits (Fig. 9). Mu values for the Yilgarn were calculated using the Abitibi-Wawa lead model of Thorpe (1999), which is applicable to the Abitibi-Wawa Subprovince and the Eastern Goldfields Superterrane (EGST) of the Yilgarn Craton (refer to Thorpe et al., 1992; Thorpe, 1999 and Huston et al., 2014, for discussions on this technique). Calculated μ values for the EGST, although covering a smaller geographic region than the Nd isotopic data, gave very comparable results to the Nd isotopic data (see Fig. 9), with both systems clearly demonstrating the spatial relationship between VHMS deposits and primitive isotopic signatures. More importantly, the finer granularity offered by the μ data showed that in the EGST, the VHMS deposits, although situated within the more isotopically primitive (juvenile) crust, were preferentially located along the margins of such juvenile zones (Fig. 9).

The close correspondence between the Nd and Pb signatures is noteworthy for a couple of reasons. Firstly, each isotope system (Sm–Nd, U–Pb) is largely providing information about different reservoirs in the crust, lower-middle versus upper crust, respectively. The close concordance, therefore, suggests that there is connectivity between these crustal reservoirs. Secondly, and perhaps more importantly, because the Pb isotope signature is being derived from ore minerals, the relationship between the Pb signature, Nd signature and VHMS mineralisation is also probably real, i.e., that the observed correlation may reflect some critical aspect of the VHMS mineral system. The latter carries the implication that isotopic signature can be used predictively for VHMS deposits in exploration targeting, i.e., an important component of the VHMS mineral system is a juvenile setting. This association also provides a possible clue as to the long-standing question of why much of the Yilgarn Craton (with a long crustal prehistory) was not as prospective for VHMS mineralisation as other Archean terranes, such as the isotopically-juvenile VHMS-rich Abitibi-Wawa Subprovince in the Superior Province.

Huston et al. (2005, 2014) investigated this further and were able to show that the relationship between juvenile (young) crustal domains (as identified by Nd and/or Pb isotopic data) and VHMS deposits was evident not just in the Yilgarn Craton but in other Archean (and, possibly, Proterozoic) terranes around the world (Fig. 10). This was best demonstrated through the relationship between fertility (tonnes of metal resource) versus isotopic signature compiled for various Archean cratons (Fig. 11). The apparent correlation of VHMS occurrences with primitive isotopic zones, identifiable in both Nd (from regional granites) and Pb (from galena), strongly suggests a causal link between juvenile crustal growth and VHMS mineralisation. Both Nd and Pb data in the high fertility domains indicate there was limited interaction with pre-existing crust. Huston et al. (2014) suggested that the isotopes are recording the favourable tectonic setting for this mineralisation in extensional zones, characterised by high-temperature juvenile magmas (and extensive structuring) and developed favourable tectonic scenarios for this mineral system. Note that FIII-type rhyolites commonly associated with Archean VHMS deposits (e.g., Lesher et al., 1986; Hart et al., 2004) would also be expected to be largely isotopically primitive and consistent with the Huston et al. (2014) model. Such rhyolites are also associated with the VHMS mineralisation in the Yilgarn Craton (e.g., Champion and Cassidy, 2007, 2008).

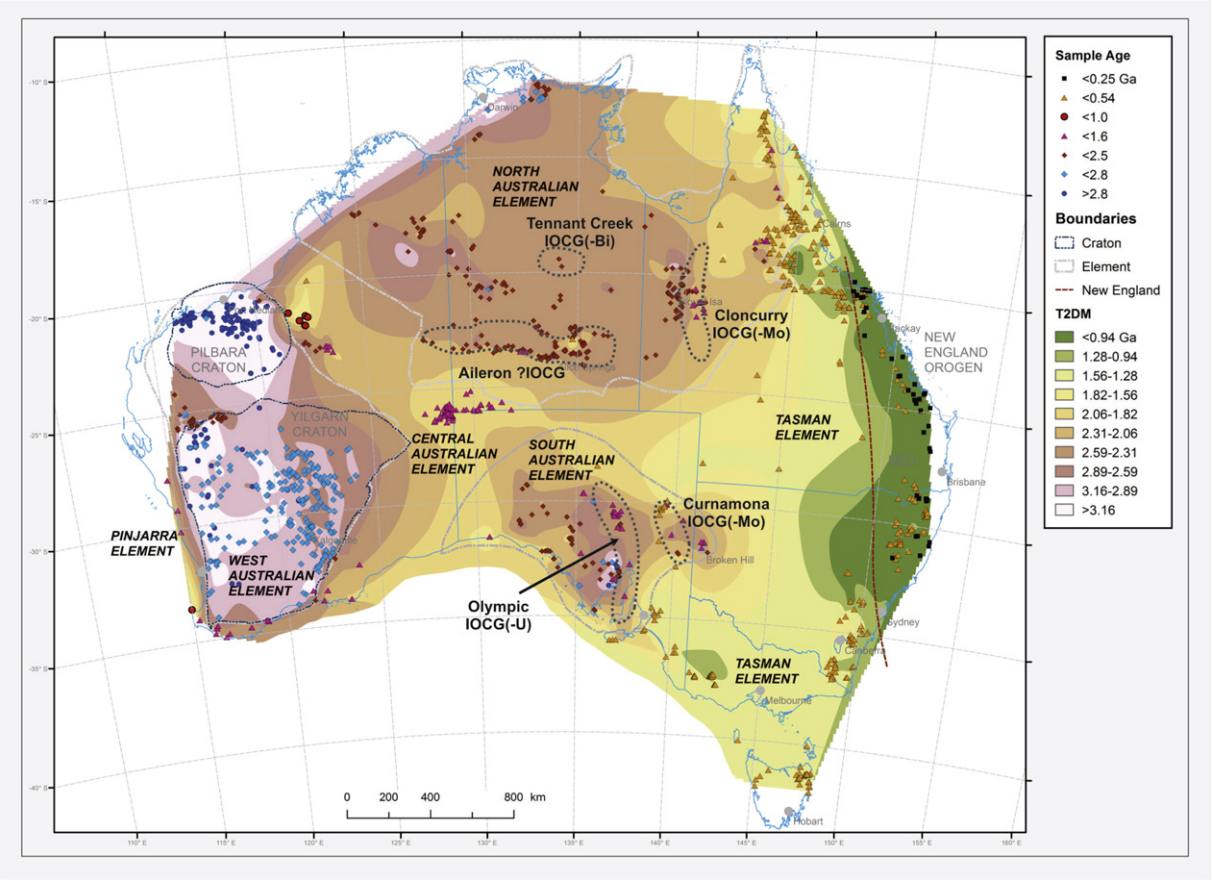

Fig. 12. Plot of iron oxide copper gold (IOCG) provinces overlain over gridded two-stage depleted mantle model age (T_{2DM}) map of Australia (Champion, 2013). Figure updated from Skirrow (2013). As noted by Skirrow (2013), there is a good correlation between these mineral provinces and apparent gradients (breaks) in the regional T_{2DM} map. Refer to Champion (2013) for Sm–Nd data sources. Element nomenclature follows Huston et al. (2012).

5.4. Iron oxide-copper-gold deposits and isotopic gradients—old continental margins?

Skirrow (2013) demonstrated a useful empirical relationship between regional isotopic zonation and a number of iron oxide copper gold (IOCG) camps in Australia, namely that many of the Australian IOCG belts have a spatial association with marked isotopic gradients (Fig. 12). Skirrow (2013) demonstrated this relationship at the continental-scale, but it also applicable at more regional scales (e.g., Fig. 13). The simplest interpretation of such gradients is that they represent an earlier accretionary continental margin environment, i.e., increasingly juvenile isotopic signature (younger model ages) towards the continental margin, e.g., south-western USA (Bennett and DePaolo, 1987); Tasman Orogen of eastern Australia (Kemp et al., 2007; Champion et al., 2010; see below). Such tectonic environments have been suggested for most of the areas highlighted by Skirrow (2013), and include Mount Isa, Korsch et al. (2011); southern Arunta, Zhao and McCulloch (1995); Scrimgeour et al. (2005); and the Gawler. An important feature of these suggested scenarios is the range of ages of the paleo-margins, e.g., for the Mount Isa and eastern Gawler, which are often placed along strike of each other in tectonic reconstructions, margins may be ca. 1.85 Ga (e.g., Payne et al., 2009; Korsch et al., 2011) or perhaps older, e.g., 1.95 Ga for Mount Isa (McDonald et al., 1997; Gregory et al., 2008); 2.5 Ga for the Gawler (e.g., Swain et al., 2005). The Arunta margin is more tightly constrained and appears to have been operative ca. 1880 Ma to ca. 1650 Ma (Zhao and McCulloch, 1995; Scrimgeour et al., 2005). As noted by Champion (2013), the isotopic data for the southern half of the Northern Territory shows a strongly increasingly primitive signature, consistent with a relatively long-lived accretionary margin, evident not just on regional model age images but also in the raw isotopic data (Fig. 14). These ages are mostly older than interpreted mineralisation ages (see Groves et al., 2010).

Notably, the association between some of Australia's IOCG camps and isotopic gradients is also evident in Pb isotopic data from galena, and other mineralised samples, from a wide range of deposit types including lode gold, a number of Pb–Zn deposit styles and IOCG deposits. Fig. 15 uses μ values calculated from the Pb isotopic data using the CSIRO-AGSO North Australian model (Sun et al., 1996; Carr et al., 2001) for deposits with Pb model ages between 2.0–1.575 Ga. Although the Nd model age map and the Pb μ map differ in detail, they are broadly similar and importantly both show that the Cloncurry IOCG belt and the suspected Aileron IOCG belt not only straddle regions marked by pronounced isotopic gradients but are elongate perpendicular to these isotopic gradients. This apparent agreement is an interesting observation, and as for Archean VHMS deposits (Huston et al., 2014), suggests that the isotopic gradients may be informing on an integral component of the IOCG mineral systems, in this case most likely identifying paleo-margins, given the interpreted geology for these regions (e.g., see Huston et al., 2012, and references therein).

This apparent association with old margins is not surprising and has been suggested by others, e.g., by Skirrow (2010), based on seismic reflection data for the Olympic Dam IOCG deposit. In a recent review of IOCGs, Groves et al. (2010) suggested that larger Precambrian IOCG deposits (>100 tonnes of resources) were located in intracratonic settings but close to (within ~100 km) of either craton margins or lithospheric boundaries (which the regional Nd and Pb isotopic patterns are successfully identifying). Groves et al. (2010) further suggested that the larger IOCGs formed shortly following supercontinent formation

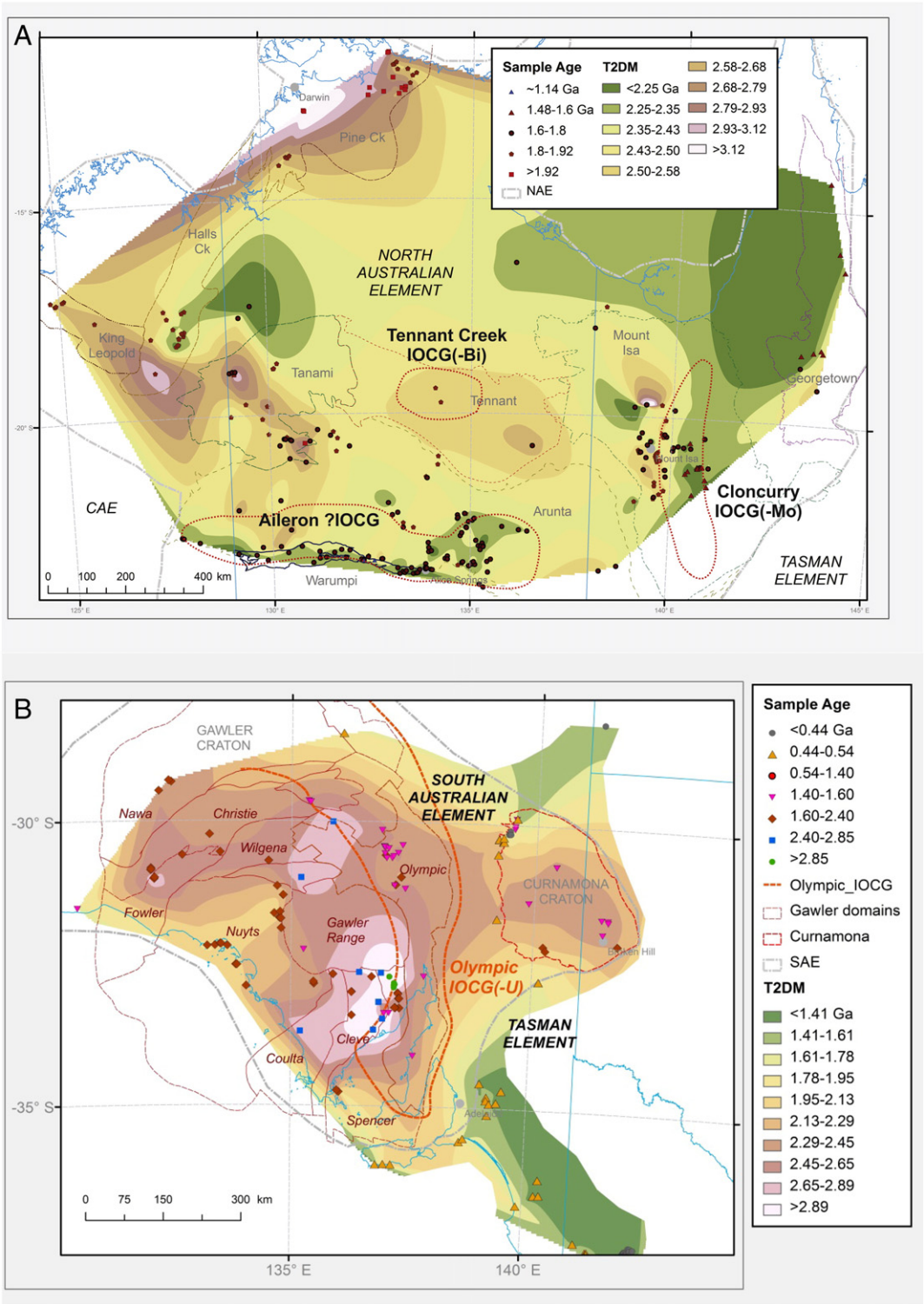

Fig. 13. Regional-scale gridded T_{2DM} map of: A) the North Australia Element, and; B) the South Australian Element, with Aileron, Cloncurry, and Olympic Dam IOCG camps superimposed. IOCG fields from Skirrow (2013). Outlines of Gawler and Curnamona Cratons and geological domains of the Gawler Craton from Ferris et al. (2002). Refer to Champion (2013) for Sm–Nd data and data sources. Element boundaries follow Huston et al. (2012). Geological province and region boundaries (Pine Creek, Halls Creek, King Leopold, Tanami, Tennant, Arunta, Warumpi, Mount Isa and Georgetown) after Stewart et al. (2013).

(100–200 Myr after) implying that age criteria can also be used for identifying potential IOCG corridors. Caution is needed, however, as this relationship in part reflects how IOCGs are classified. Interpreted IOCG deposits in Tennant Creek, Northern Territory, for example, which Groves et al. (2010) interpreted as high grade Au (+Cu) deposits not true IOCGs, were generated during Nuna formation not afterwards (e.g., Huston et al., 2012);

Given the apparent preferred location of IOCGs close to craton margins/sutures, Groves et al. (2010) postulated a role for (subduction-related) metasomatised lithospheric mantle and presented a mineral system model whereby partial melts of this lithosphere transported Cu, Au and volatiles into the crust (although local country rocks have also been suggested to supply elements including uranium, e.g., Olympic Dam, Skirrow et al., 2007). Such lithospheric melts

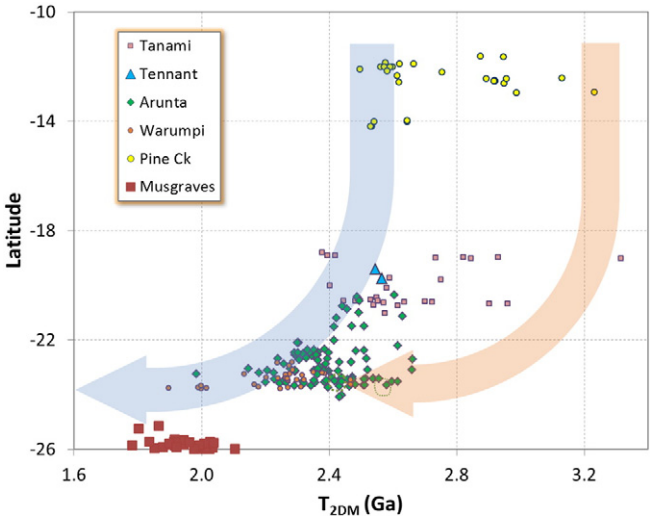

Fig. 14. Two-stage depleted mantle model (T_{2DM}) ages versus latitude for felsic igneous rocks of the Northern Territory. Note the general decrease in minimum and max T_{2DM} with decreasing latitude, highlighted by the blue and orange arrows, respectively. This is particularly evident south of latitude 20°. Figure modified from Champion (2013); refer to that reference for Sm–Nd data and data sources.

would certainly be expected to be oxidised (e.g., Rowe et al., 2009) and have the potential for elevated gold solubilities (e.g., Jégo et al., 2010). Such rocks may also have contributed copper. Gregory et al. (2008), on the basis of Re–Os isotopic data, have suggested that melts derived from metasomatised lithosphere may have been the source of copper in the Mount Isa ore body. The presence of igneous rocks, potentially derived from metasomatised lithosphere, could be used in conjunction with the isotopic maps to further highlight areas of potential for IOCG deposits. Interestingly, melts of such metasomatised lithosphere would in themselves not necessarily have juvenile isotopic signatures, depending on both the timing of metasomatism and the role of sediments (if any) in the subduction component responsible for metasomatism. A potential example is the Tasmanian Jurassic dolerites which Hergt et al. (1989) interpreted as being derived from subduction-related metasomatised mantle lithosphere and which have very evolved isotopic signatures (e.g., ε_{Nd} of −6). Finally, it should be noted that although both Johnson and McCulloch (1995) and Skirrow et al. (2007) suggested, on the basis of Sm–Nd isotopes and correlations with Cu contents, that juvenile mantle melts (thought to be either alkaline mafic or ultramafic melts, produced during the Hiltaba Suite magmatism) were the source of at least some of the copper at the very large Olympic Dam deposit, there is no compelling evidence that these are lithosphere melts For example, the recent review of Arndt (2013) points out the low likelihood that large volumes of melt can be generated from such sources. This does not, however, change the apparent empirical relationship between Nd (and Pb) isotopic signatures and IOCG belts as pointed out by Skirrow (2013); Fig. 12).

Another way the isotopic data can be utilised with regards to IOCGs is by looking at maps of crustal residence (T_{Res}) which give an indication of the residence time of various parts of the crust. This approach is very applicable to the Gawler Craton where there is a wide spread granites of similar age or not significantly older (ca. 1860–1570 Ma) than the accepted age of IOCG mineralisation (ca. 1600–1570 Ma; Skirrow et al., 2007). The crustal residence map provides a snap shot of what the crust (and lithosphere) of the Gawler Craton may have looked like at the time the IOCG deposits in that area were forming (Fig. 16). From that figure it is clear that the isotopic data are consistent with continental margins on both sides of the Gawler Craton at varying times, and the geology has been interpreted to indicate a convergent margin setting on the southwestern part of the Gawler Craton at ca. 1630–1610 Ma (e.g., Swain et al., 2008) and probably also ca. 1700 Ma (Ferris and Schwarz, 2004; Payne et al., 2010). This begs the question

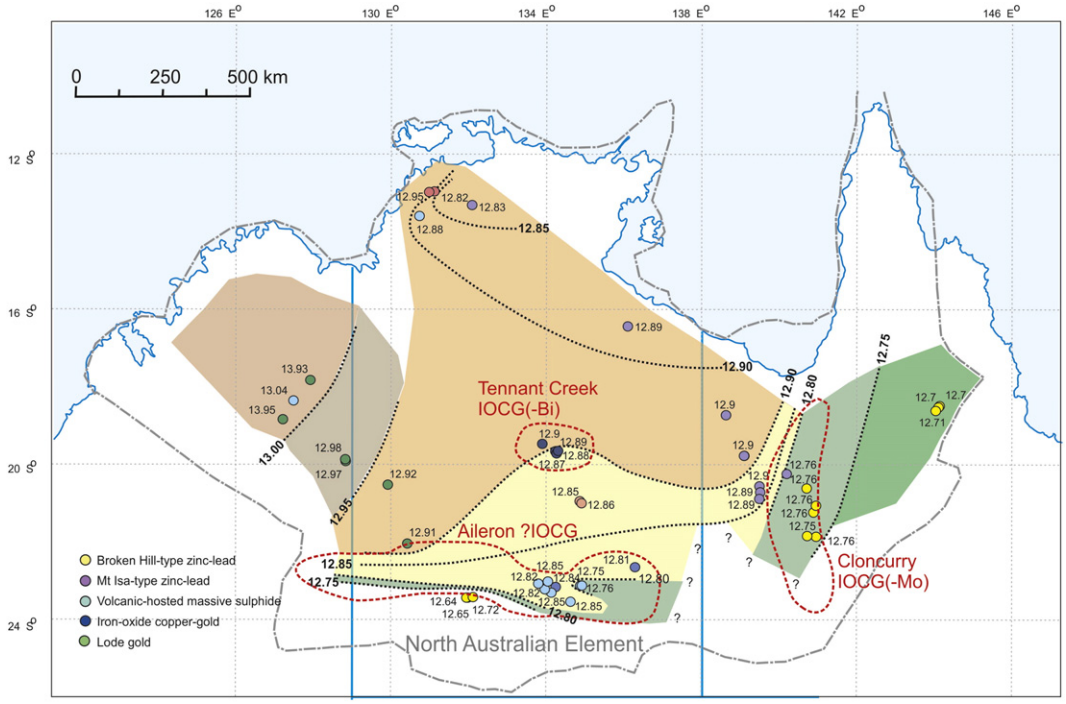

Fig. 15. Variation in mu ($\mu = {}^{238}U/{}^{204}Pb$) of Paleoproterozoic and Mesoproterozoic Zn–Pb, lode gold and IOCG deposits in the North Australian Element. Mu values calculated from the CSIRO-AGSO North Australian model (Sun et al., 1996; Carr et al., 2001) for deposits with Pb model ages between 2.0 and 1.575 Ga (mostly 1.81–1.64 Ga). Lead isotopic data from Warren et al., 1995; Sun et al., 1996; Black et al., 1997; Carr et al., 2001; Hussey et al., 2005; Kositcin et al., 2009; D. Huston, unpublished data) (mostly) high precision (double spike or ICP-MS) analyses. Figure modified from D. Huston (unpublished), with IOCG camps (Skirrow, 2013) superimposed. Outline of North Australian Element from Huston et al. (2012).

of why IOCG mineralisation is localised on the eastern and northeastern margins of the Gawler Craton. It could be speculated that the answer has something to do with the suggestions of Groves et al. (2010) that specific earlier events, either with some specific characteristic or age (e.g., 100–200 Myr after supercontinent formation), may have something to do with controlling mineralisation. It could also be speculated, however, that the mineralisation may in part reflect lithospheric focussing of mantle-derived melts such as those suggested by Begg et al. (2010) for Ni deposits, and there is perhaps some evidence for this (see below). Skirrow (2010) suggested an intermediate model for Olympic Dam, with delamination (resulting from lithospheric thickening caused by orogenic processes to the east) localised along but not within Archean lithosphere, resulting in mafic and ultramafic magmatism, caused by, and focussed into, the delaminated region, and which was ultimately responsible for mineralisation.

In addition to T_{Res} maps, similar images can be produced for a particular time slice using model age maps constructed for a specific time slice, e.g., for 1800 Ma the model age is calculated as follows:

$$T_{2DM(1800\ Ma)} = T_{2DM} - 1800; \text{ for all } T_{2DM} \text{ greater than } 1800\ Ma.$$

In regions where the magmatism has a restricted age range this will produce images that are similar to the T_{Res} maps. In regions with a large range of magmatic ages, such maps will be different and pseudo-time slices based on Nd model ages can be produced (see Fig. 17A, B and C).

The Gawler Craton is particularly amenable to such an approach as felsic magmatism there spans more than 1500 Myr (e.g., Reid and Hand, 2012). Fig. 17 readily illustrates a number of points relative to the location of the Olympic IOCG belt. Firstly it is clear that the belt straddles the margin of the 2500 Ma and older crust (as defined by the presently available isotopic data). Secondly, there is evidence in the 2500 Ma and younger time slices, of marked isotopic zonation along this margin, e.g., the old crustal block in the south and the juvenile embayment in the north. The former appears to largely have no relevance to the position of the IOCG belt. However, the juvenile embayment overlaps regionally with, and is evidence for more juvenile crust around the world-class Olympic Dam deposit (the largest IOCG deposit in the region; Fig. 17). This zone could represent a long-lived juvenile feature (possibly dating back to the Archean though the number of samples at this time is limited) but is more likely to reflect juvenile crustal growth post-Archean, probably either at ca. 1850 Ma and/or at ca. 1590 Ma close to the time of the deposit formation (e.g., Skirrow et al., 2007). The latter is consistent with the models of Johnson and McCulloch (1995); see also Campbell et al., 1998) that suggest at least some of the metal endowment at the deposit is related to (isotopically juvenile) mafic and/or ultramafic magmas, such as those that occur within the deposit or those associated with the nearby extensive Gawler Range Volcanics (Hiltaba Suite).

Further support for such contemporaneous mantle input is evident in the felsic intrusive rocks of the widespread Hiltaba Suite magmatism (ca. 1595–1570 Ma) which become increasingly more A-type, i.e., higher temperature suggestive of greater extension and/or mantle input, towards the deposit (Budd, 2006). This higher temperature zone corresponds to a region of lithospheric thinning in the model of Skirrow (2010). As noted by Campbell et al. (1998), the metal source could be either directly derived from contemporaneous mafic/ultramafic magmatism or leached from such pre-existing rocks. Both would only be fully consistent with the model of Groves et al. (2010) if the mafic/ultramafic magmatism was derived (at least in part) via partial melting of the lithosphere (as

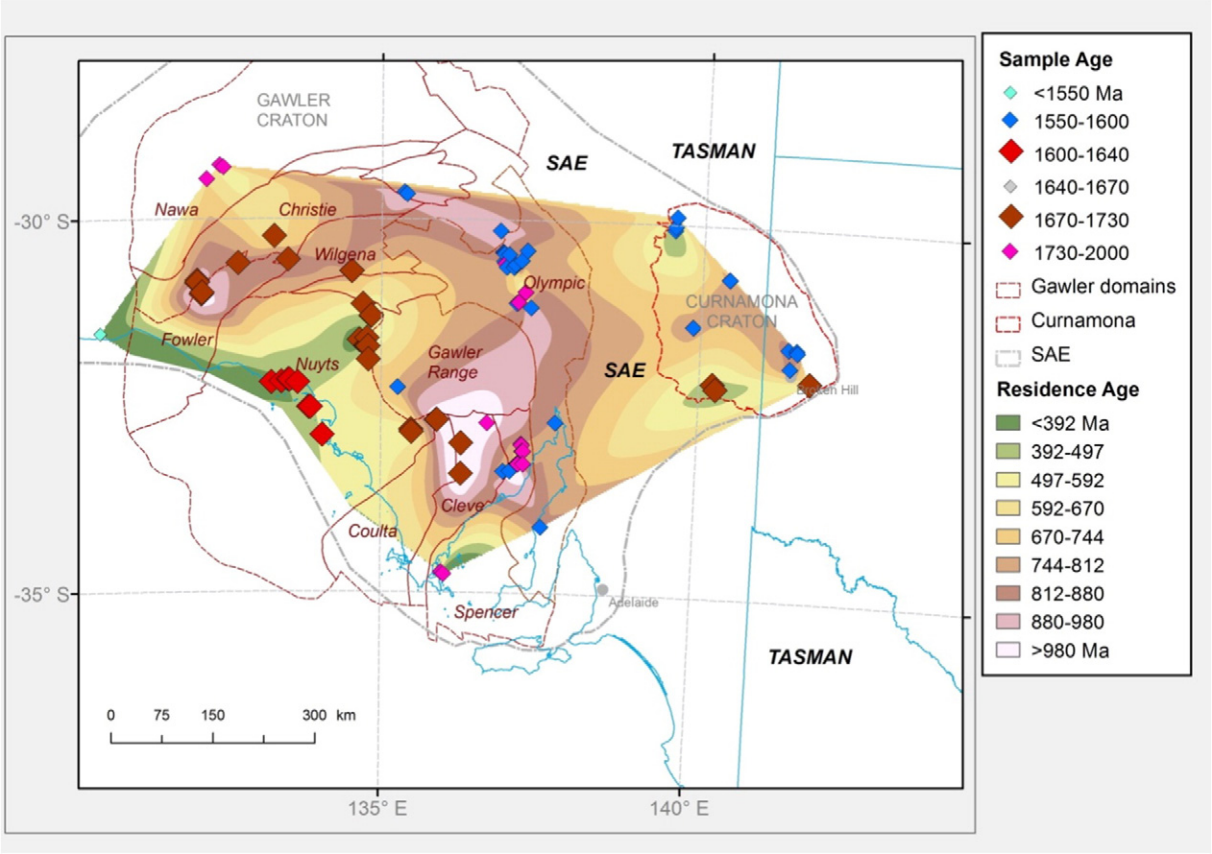

Fig. 16. Crustal residence age map for the Gawler Craton, based on T_{Res} of ca. 2000–1550 Ma granites from that craton. Outlines of Gawler and Curnamona Cratons are also shown as are the geological domains of the Gawler Craton (from Ferris et al., 2002). Refer to Champion (2013) for relevant data and data sources.

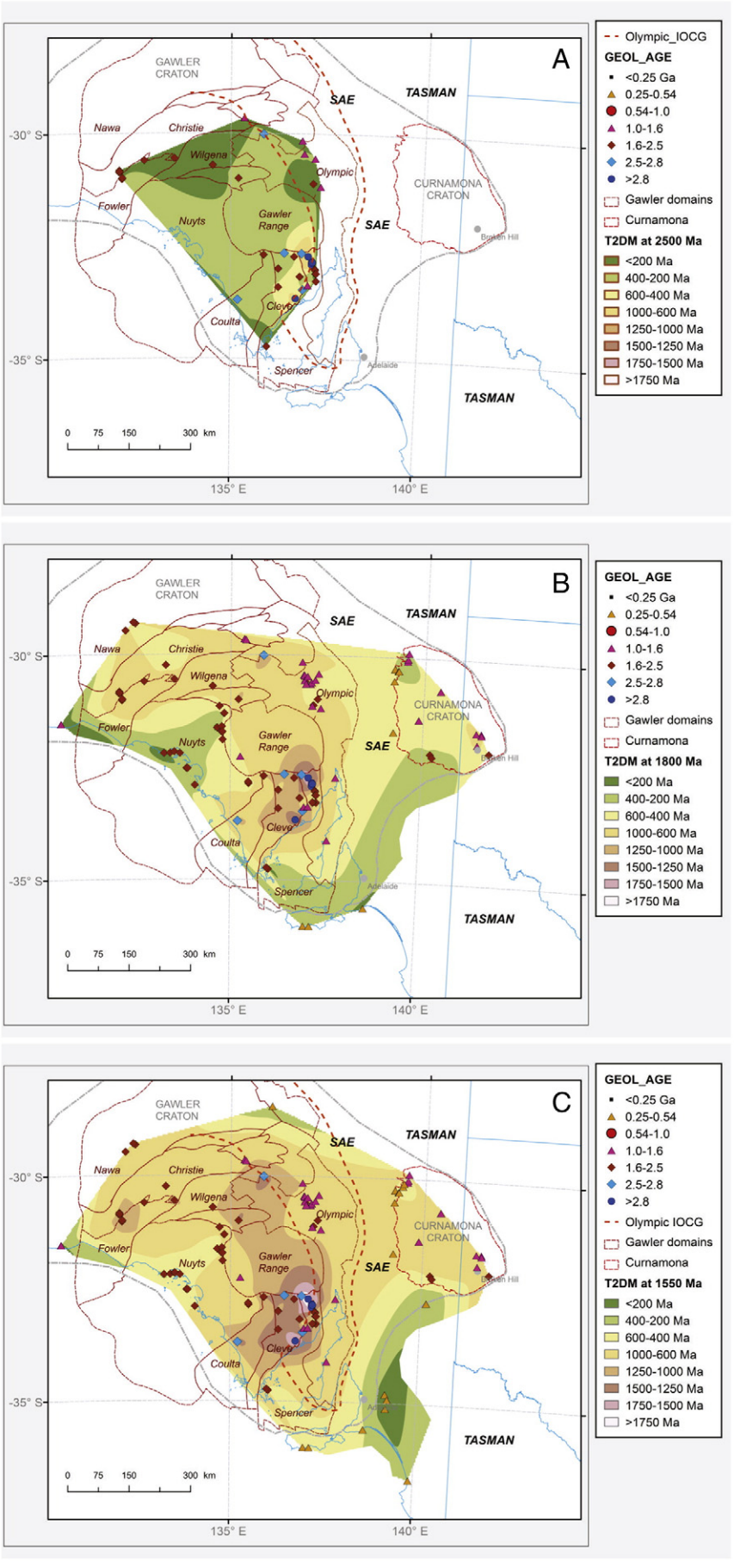
A
GAWLER CRATON
SAE
TASMAN
CURNAMONA CRATON
Nawa
Christie
Wilgena
Olympic
Fowler
Nuyts
Gawler Range
Cleve
Coulta
Spencer
Adelaide
Broken Hill
-30° S
-35° S
0 75 150 300 km
135° E
140° E
Olympic_IOCG
GEOL_AGE
<0.25 Ga
0.25-0.54
0.54-1.0
1.0-1.6
1.6-2.5
2.5-2.8
>2.8
Gawler domains
Curnamona
T2DM at 2500 Ma
<200 Ma
400-200 Ma
600-400 Ma
1000-600 Ma
1250-1000 Ma
1500-1250 Ma
1750-1500 Ma
>1750 Ma
B
T2DM at 1800 Ma
C
T2DM at 1550 Ma

discussed earlier). Both would also be at least partly consistent with models such as those of Begg et al. (2010), i.e., mafic–ultramafic magmatism being favourably focussed into the region around the giant Olympic Dam deposit. The 1550 Ma time slice (Fig. 17C), like the T_{Res} image (Fig. 16), provides a reasonable approximation to what the crust was like at the time of widespread Hiltaba magmatism, and IOCG mineralisation.

5.5. Predictive analysis based on radiogenic signatures: Granite-related mineralisation

Significant advances in controls of granite-related metallogeny have been made since the landmark papers of Ishihara (e.g., Ishihara, 1977, 1981) who recognised the important controls the redox state has on granite magmas and resulting mineralisation styles. This work was extended by Blevin and co-workers (Blevin and Chappell, 1992; Blevin et al., 1996; Blevin, 2004), who showed that factors such as the degree of chemical evolution of the granite also had important controls on mineralisation styles (Fig. 18). More recently, Thompson et al. (1999) came to similar conclusions (Fig. 18) and added a tectonic interpretation. The latter shows, unsurprisingly, that more-lithophile elements such as tin (Sn), molybdenum (Mo) and tungsten (W) are associated with continental material in backarc and arc-rift or non-arc extensional environments, in contrast to chalcophile Cu and Cu–Au mineralisation, which they suggested were related to more primitive crust, e.g., island arcs, primitive continental arcs (consistent with the oxidised nature of arc rocks, e.g., Parkinson and Arculus, 1999).

Consideration of these simple relationships suggest isotopic data, such as Nd, would be best at delineating potential regions for porphyry Cu and Cu–Au mineralisation (i.e., regions with more juvenile isotopic signatures). A good example of this association in Australia is the Ordovician–earliest Silurian Cu–Au mineralisation associated with isotopically juvenile magmatism in the Macquarie Arc, in central New South Wales (e.g., Cooke et al., 2007; Fig. 19). These rocks are readily identifiable in both the regional- and national-scale Nd model age maps and T_{Res} maps (Fig. 19), even though there are only a few points in the data set. Huston et al. (2016-in this volume) show that these juvenile crustal domains in New South Wales, and their associated Cu–Au mineralisation, are also clearly evident in Pb isotope maps. The latter maps were produced from Pb isotopic data from galena and other Pb-rich samples from a range of mineral deposits in New South Wales. Isotopic data was gridded using the calculated degree of mixing between crustal and mantle reservoirs based on the plumbotectonic model of Carr et al. (1995). The close agreement between the Sm–Nd data (from felsic magmatic rocks) and the more extensive U–Th–Pb data (from mineralised samples) is noteworthy, and like that found for Archean VHMS deposits (Huston et al., 2014), demonstrates a clear link between different parts of the lithosphere for the porphyry Cu–Au mineral system in this (and other) regions.

Another potential eastern Australian example of the link between juvenile isotopic domains and porphyry Cu–Au mineralisation is in the region of the Mount Morgan deposit in central Queensland (Fig. 19). The Cu–Au mineralisation at Mount Morgan is associated with rocks thought to be related to either a primitive continental arc (e.g., Morand, 1993) or island arc (Calliope Gamilaroi arc, e.g., Murray and Blake, 2005), although the mineralisation style is controversial. However, although the associated magmatic rocks are isotopically primitive, they are not readily discriminated in the gridded Nd model age data as they fall within the isotopically primitive young rocks of the New England Orogen. They are, however, clearly visible on images displaying Nd residence maps (Fig. 19), illustrating the importance of secular as well as spatial variations in isotopic systematics. Other regions with potential for such deposits in Australia can be suggested. These include the Ordovician rocks of the Netherwood region in north Queensland (southwest of Cairns on Fig. 19), and Proterozoic rocks in the Warumpi Province (in the North Australian Element, Fig. 13A) and Nuyts Domain, Gawler Craton (Fig. 16). All of these are in or close to regions suggested to have a tectonic history including island arcs (e.g., Scrimgeour et al., 2005; Swain et al., 2008; Henderson et al., 2011). All are readily evident on regional gridded images even where the numbers of analysed samples is low. These regions are also easily identifiable in other isotopic figures, e.g., ε_{Nd} versus time (see Champion, 2013). Of course, Nd (and other isotopic) data only identify the locations of potentially juvenile terranes; they do not convey any information on additional important factors, such as depth of current crustal exposure (and degree of preservation of porphyry and epithermal mineralisation). It is also noted that Cu–Au mineralisation styles are also found in continental arcs though the delineation of these on the basis of their isotopic signature is more problematical given the non-unique isotopic signature of such rocks.

Unfortunately, felsic magmatic rocks associated with Sn, W and intrusion-related gold mineralisation have a demonstrably wide range of isotopic signatures (from juvenile to evolved), and metallogenic terranes with such mineralisation can not easily be identified from isotopic data. Blevin et al. (1996) and Champion et al. (2010) clearly showed this for Sn- and IRG-associated granites of the New England Orogen and north Queensland region, whose isotopic signatures range from ε_{Nd} of $+5$ (and over) to -7 (and lower), respectively. Champion et al. (2010) showed that magmatism associated with Sn mineralisation in both regions is of very similar chemistry despite the large isotopic differences.

5.6. General comments and conclusions

Isotopic maps can also be used with other processes thought to be important in mineral systems, such as those that relate mineralisation styles to tectonic settings, such as continental arcs, backarcs etc. One simple example is the identification of possible accretionary orogens and their associated mineralisation, such as gold, copper-gold (e.g., Hronsky et al., 2012). One indicator of accretionary margins in isotopic data (and useful for exploration targeting), is a strong trend to increasingly juvenile isotopic signatures with both geography and age, as exemplified in the western United States (e.g., Farmer and DePaolo, 1983; Bennett and DePaolo, 1987) and (the Tasman Element of) eastern Australia (e.g., Kemp et al., 2009; Champion, 2013; Fig. 12). Recently, Collins et al. (2011) have expanded on this and suggested that different types of orogenic systems (External = dominantly accretionary, e.g., circum-Pacific, versus Internal = dominantly collisional, e.g., Europe) can also be discriminated on the basis of isotopic signature. We agree with this in general although the results of Champion (2013) indicate that the isotopic signature for 'Internal' or collisional orogens is non-unique (Table 3). Collins et al. (2011) used Lu–Hf isotopic signatures from in-situ measurements in zircon, which has the advantage of being able to detect isotopic components in a magmatic rock. Their results, however, are also transferrable to other isotopic systems, especially whole rock Sm–Nd (as long as there is sufficient Nd whole-rock data to sample the range of isotopic signatures within a region, e.g., compare Sm–Nd and Lu–Hf plots in Kemp et al., 2009).

Fig. 17. Model age time slice figures (A: at 2500 Ma; B: at 1800 Ma; C: at 1400 Ma) for the Gawler and Curnamona Cratons of the South Australian Element, Australia. The Olympic IOCG field (from Skirrow, 2013) is denoted by orange dashed line in A and C. Note the persistent more juvenile isotopic embayment located around the Olympic Dam IOCG deposit (near the word 'Olympic' on A, B and C). Refer to Champion (2013) for Sm–Nd data and data sources.

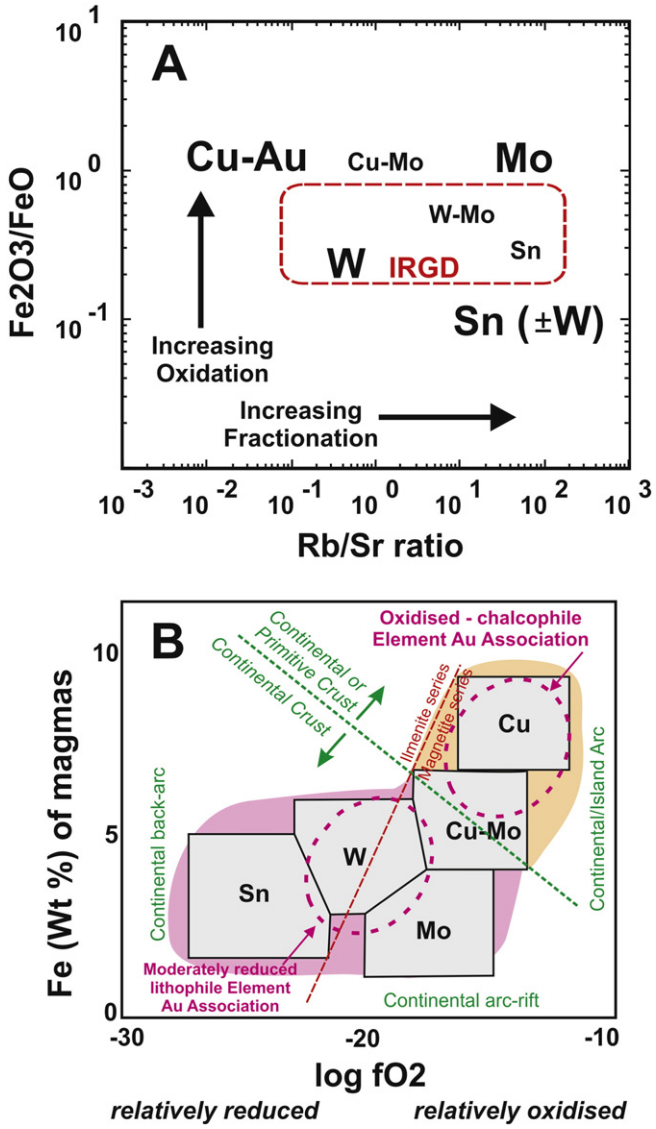

Fig. 18. (A) Rb/Sr ratio versus Fe_2O_3/FeO ratio plot of Blevin et al. (1996). The plot illustrates the relationship between the degree of oxidation and compositional evolution of the magma (based on whole-rock compositions) and the dominant commodities in related mineralisation. Intrusion related gold deposit (IRGD) field from Blevin (2004). (B) Plot of oxygen fugacity versus amount of total Fe in the magma, also showing tectonic setting. Plot modified after Thompson et al. (1999) and Lang et al. (2000).

Based on these analogies, the regional isotopic variation evident in the southern North Australian Element (e.g., Champion, 2013; Figs. 13 and 14) suggests an accretionary margin origin and, thus can be considered to have potential for arc- and backarc-related mineralisation (in addition to the IOCG mineralisation discussed earlier). Both the Sm–Nd and U–Th–Pb isotopic data for this region shows a southward increase to more juvenile compositions (e.g., decrease in Nd model ages and μ values) over a significant geographic extent (~400 km; Figs. 15 and 13). Geological evidence for an accretionary margin, however, is largely confined to the southern part only, in the southern Aileron (e.g., Zhao and McCulloch, 1995) and Warrumpi Provinces (e.g., Scrimgeour et al., 2005; Ahmad and Scrimgeour, 2013). The calc-alkaline trondhjemite suite of Zhao and McCulloch (1995), for example, is interpreted to represent part of such an arc within the southern Aileron Province.

The mismatch between the isotopic signature and geology raises the question of whether or not older accretionary margins exist to the north obscured by younger rocks. Notably, Korsch et al. (2011) suggested, based on seismic reflection data, that there is an ancient crustal suture (expressed at the surface by the Atuckera Fault) between the Aileron Province and provinces to the north. They linked this suture to a similar break observed between the Tanami region and the Aileron Province to the northwest (documented by Goleby et al., 2009). Bagas et al. (2008) proposed a collisional event between the Tanami and Arunta region occurring ca. 1850 Ma. Goleby et al. (2009) and Korsch et al. (2011) suggested a similar scenario. This simple example, although speculative, shows that a range of arc- and backarc-related mineralisation styles may potentially extend significantly to the north in this region (albeit probably under cover). The location of the Tennant Creek IOCG mineral deposits may also be consistent with this scenario if models such as those of Groves et al. (2010) are correct (see earlier discussion).

Through a range of simple examples we have attempted to illustrate how regional and continental scale isotopic maps (and data) can be used to empirically and/or predictively identify (either directly or indirectly by proxy), larger scale parts of mineral systems that may be indicative, or form part of, metallogenic terranes, for a variety of mineral systems. Of course, in any exploration model, be it based on the mineral systems concept or otherwise, any analysis is predicated on using a wide range of geological, geochemical and geophysical information across a range of scales (see discussion by McCuaig et al., 2010). Isotopic maps, such as the Sm–Nd and U–Th–Pb images presented here, are just another layer to be integrated with other data. One simple example would be integration of the isotopic data with major crustal boundaries interpreted from geophysical data, such as the Australian compilation of Korsch and Doublier (2016-in this volume) based on seismic reflection data.

6. Discussion and future developments

6.1. In-situ analysis of radiogenic isotopes

Advances in in-situ analysis of radiogenic isotopes in the last two decades (e.g., Stern, 1999) have led to a number of innovative approaches to investigating metallogenesis. With regards to the approaches outlined in this paper, the in-situ U–Pb and Lu–Hf analysis of zircons (especially when analysed concurrently, e.g., Fisher et al., 2014), provides the ability to look at inherited components and allows the potential characterisation of secular changes in crustal and lithospheric growth based on these inherited components. A good example of this is provided by Mole et al. (2014) who investigated Lu–Hf signatures (and U–Pb ages) of inherited and xenocrystic zircons in granites of the Yilgarn Craton of Western Australia. From this data they were able to provide a series of temporal snapshots (at 3050–2820 Ma, 2820–2720 Ma and 2720–2600 Ma) of crustal growth that suggested the craton was built up from a series of Archean micro-continental blocks. This is a particularly valuable approach, even more so for regions like the Yilgarn Craton which are dominated by magmatism of broadly one age range (ca. 2.75–2.63 Ga; Cassidy et al., 2002). These temporal maps allowed the investigation of the relationship between ca. 2.9 Ga and ca. 2.7 Ga komatiite occurrences and paleo-crustal structure and extension of the Begg et al. (2010) model back in time. Not surprisingly the ca. 2.7 Ga craton margin from Mole et al. (2014) based on Lu–Hf data closely matches that outlined by the Sm–Nd whole rock data (Champion and Cassidy (2007, 2008), though Mole et al. (2014) were able to identify another crustal block in the southwest part of the craton (an area with poor Sm–Nd data coverage).

The methodology of Mole et al. (2014) is also clearly an advance on temporal snap shots compiled from isotope model ages alone, such as shown in Fig. 17, as the former is not affected by complexities such as younger crustal growth, magma mixing and other contemporaneous juvenile input. The approach is not without problems though. One of the potential criticisms is that it does not discriminate between zircons that are truly representative of the crust in the general area of the host intrusive and those that are exotic to the area. The main problem here are detrital zircons, either introduced as xenocrysts from sedimentary

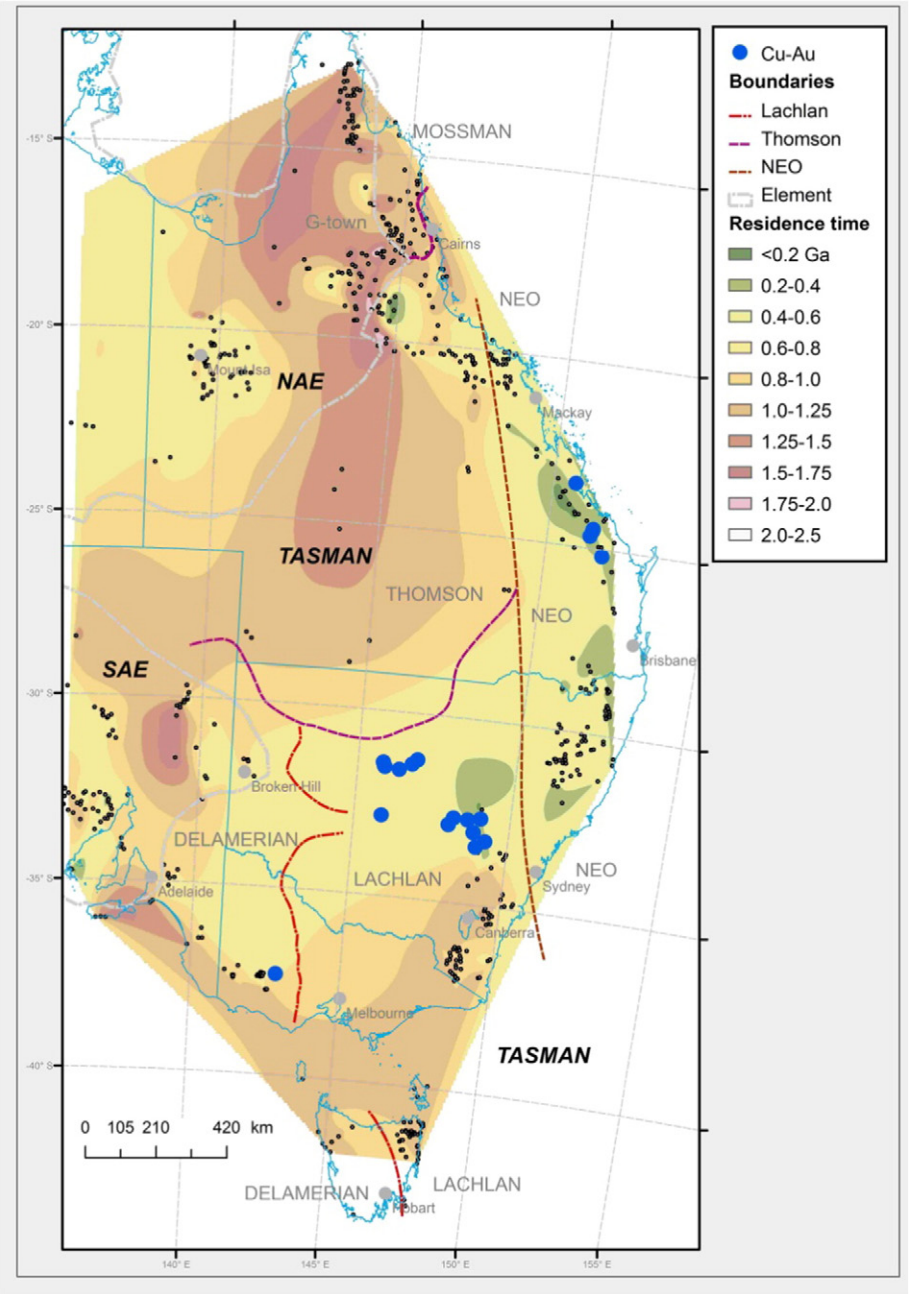

Fig. 19. Location of copper-gold deposits superimposed on the gridded Nd residence age map for the Tasman Element and surrounding regions (South (SAE) and North (NAE) Australian elements). Copper-gold deposits (from the Australian Mines Atlas; http://www.australianminesatlas.gov.au/) are shown as blue circles. Also shown are the Delamerian, Lachlan, Thomson and Mossman orogens of the Tasman Element. There is a good correlation between many copper-gold deposits and zones with young residence ages, notably in the central Lachlan Orogen and the central New England Orogen. Copper-gold deposits outside of these two zones are almost exclusively not magmatic-related. Location of Nd samples used to create the grid are shown as black circles. Data and data sources are given in Champion (2013). Boundaries of Delamerian, Lachlan, Thomson, Mossman and New England (NEO) orogens modified from Stewart et al. (2013).

rocks the granite has interacted with or perhaps part of the source region (i.e., local contribution from melted sediments), i.e., the isotopic signature of the zircon in question has been brought in laterally from elsewhere. As discussed by Champion (2013) this is probably less of a problem in the Archean, especially the Yilgarn Craton, where sedimentary rocks are not a large component of the geology (unlike say eastern Australia, e.g., Kemp et al., 2009), but can be more problematic, especially when it is considered how far zircons can be recycled (e.g., Sircombe, 1999). The additional use of oxygen isotope analysis on the same zircons provides one solution as it allows identification of, and thus avoidance of, zircons (via their elevated delta ^{18}O ($\delta^{18}O$)) that have grown in material that is partly or totally derived from supracrustal sources, i.e., have experienced low temperature processes (e.g., Valley et al., 2005). This approach does not distinguish transported zircons with a mantle-like $\delta^{18}O$, from local zircons with a mantle-like $\delta^{18}O$, however. It should be noted that the potential involvement of sedimentary components is also a problem for the whole rock Nd maps described earlier. The approach of Mole et al. (2014), especially when combined with oxygen isotope data, is clearly an area of extensive possibilities utilising the approach outlined here, especially given the great, and increasing, volume of in-situ Lu–Hf analysis, and increasing amounts of accompanying oxygen isotope data now being collected.

6.2. Complementary isotopic systems: Mapping and linking different parts of the lithosphere

Isotopic studies have significant potential to investigate linkages between mineralisation and the relative roles (and importance) of various parts of the lithosphere, not just as tracers for fluid or metal sources but also, as demonstrated here, as indicators of geological setting, crustal and lithospheric architecture, geodynamic environment and/or processes, zones of greater permeability (for crustal or mantle melts), and other proxies/indicators of mineral systems. In this contribution we have largely concentrated on isotopic maps based on Sm–Nd (and by similarity Lu–Hf) from felsic magmatic rocks and U–Th–Pb from galena and Pb-rich mineralised samples. These provide some indications of possible linkages between crustal architecture and mineralisation but more could be done. An obvious first step to better link the U–Th–Pb system in mineralised samples to Sm–Nd from granites, for example, would be by investigating U–Th–Pb systematics of the felsic igneous rocks themselves, for example, Wooden et al. (1998) linked the U–Th–Pb signatures of granites to other isotopic systems, and Zartman (1974), linked signatures of felsic magmatism and mineralisation. Such linkage also allows the investigation of regions where regional patterns from U–Th–Pb in mineralised samples differ from those from Sm–Nd (or Lu–Hf) in granites, as is evident, for example, in parts of the Pilbara Craton (Figs. 5 and 4).

Another avenue for further work is to extend the approach here to other isotopic systems and sample media (including in-situ analysis of minerals) to investigate links of mineralisation to lithospheric controls. As shown in Fig. 1 mineral systems can involve the whole lithosphere (as well as the asthenosphere). Accordingly, it is pertinent to attempt to map the whole lithosphere, including the mantle component, as undertaken by Begg et al. (2009) for the African continent. Accordingly, future work should focus on characterising the whole lithosphere, including use of multiple isotopic systems on multiple rock types and minerals, in conjunction with geological and geophysical data. Such an approach can be undertaken at a range of scales. Bekker et al. (2009) and Fiorentini et al. (2012), for example, showed that multiple sulphur isotope data from sulphides can be used for exploration at the district- and camp-scale.

At the larger scale, significant advances have been made in the last decade on the geophysical mapping of the lithosphere, including the lithospheric mantle, using a variety of techniques (e.g., seismic velocity, tomography, magnetotelluric) at a range of scales, up to and including continental-scale (e.g., Australia: Kennett and Salmon, 2012; Kennett et al., 2013; North America: USArray http://www.usarray.org/(last accessed 18-Nov.-2014); and beyond (e.g., Priestley and MacKenzie, 2013). Importantly, however, geophysical images record the present-day, and are not a snap shot of previous times. As shown by Begg et al. (2009) for the African continent, the full use of such geophysical data requires integration with other data sets, such as temporal, geochemical and independent lithological information. This means not just dating parts the lithosphere (often provided by younger events) but also maximising interpretation of the lithosphere by use of isotopic and other parameters (e.g., O'Reilly and Griffin, 2006; Griffin et al., 2013).

One obvious approach to constrain evolution of the lithospheric mantle, and allow greater linkage with other isotopic systems, their respective reservoirs, and with mineralisation, is by incorporation of the Re–Os system. Re–Os isotopes can be used to provide constraints on growth and nature of the lithospheric mantle and also as a direct isotopic tracer in sulphides from ore deposits (e.g., Shirey and Walker, 1998; Carlson, 2005). The ability to temporally constrain the structure and evolution of the mantle lithosphere is important for linkage with the crustal and upper-crustal parts of the lithosphere (as effectively sampled by Sm–Nd and U–Th–Pb systems as discussed earlier). Gregory et al. (2008), for example, were able to link copper mineralisation at the Mount Isa deposit with earlier metasomatised mantle lithosphere probably related to a previous subduction environment—a paleo-margin close to that identified by both the Sm–Nd and U–Th–Pb data (Figs. 15 and 13. There are numerous other examples of interpreted model ages for mantle lithosphere using the Re–Os system (including both mantle model ages and model depletion ages (T_{RD})) often directly measured on lithospheric mantle samples (rocks and minerals; e.g., Pearson et al., 1995; O'Reilly and Griffin, 2006). The availability of such samples, however, is geologically limited and so future progress will depend largely on fuzzy and interpreted (partly unreliable) inferences derived from more extensive proxies such as mantle-derived magmas (such as the example of Gregory et al., 2008).

Although the Re–Os system has a number of characteristics which make it very amenable for studying mantle rocks (Shirey and Walker, 1998; Carlson, 2005), a variety of isotope systematics can be used for this. Price et al. (2014), for example, delineated lithospheric breaks in southeastern Australia using $^{87}Sr/^{86}Sr$ signatures of basalts. There are a number of potential difficulties with this approach, however. For example, in the study of Price et al. (2014) it is not clear if the regional changes in isotopic data are due to mantle lithosphere or crustal input. Similarly, what part of an isotopic (and geochemical) signature of mantle melts reflects mantle lithosphere or sub-lithospheric mantle variability (let alone crustal input) is difficult to resolve and controversial. Isotopic maps of the crust, such as those presented here, complement (and in part are directly related to) lithospheric age maps, e.g., Begg et al. (2010), and assuming no decoupling of crust and mantle lithosphere are expected to probably be largely similar (if not identical), at least in regard to mapping major breaks and other lithospheric architecture.

There are additional reasons to map the lithospheric mantle that are important to mineral systems, such as mapping the timing and extent of metasomatism of the lithospheric mantle. There is an argument for the critical involvement of metasomatised lithospheric mantle (either by direct melting or through contamination of asthenospheric melts), as important suppliers of ore metals or volatiles in certain mineral styles, e.g., Ni, PGE, IOCG, porphyry Cu–Au, and Th-REE deposits, e.g., Zhang et al. (2008), Groves et al. (2010), Hronsky et al. (2012), Griffin et al. (2013). Zhang et al. (2008) took this approach further suggesting that flood basalt-related mineralisation was mostly commonly related to those plumes which had not only reacted with metasomatised lithosphere but which were also emplaced within or marginal to crustal blocks of either Archean and/or Paleoproterozoic age, i.e., related to ancient metasomatism. Griffin et al. (2013) extended this further to include subduction-related metasomatism of the mantle lithosphere and later reworking of this lithosphere for a variety of deposit types. The role, if any, of metasomatised mantle, however, is controversial, and may be minimal, e.g., see the extensive arguments against it in Arndt (2013), though Arndt conceded that (REE, Th, U) mineralisation related to low-volume alkalic and/or carbonatitic magmas may have a less disputed lithospheric mantle origin.

If the involvement of metasomatised lithosphere is correct (or at least partly correct), for large-igneous province-related mineralisation, subduction-related mineralisation etc., then it follows that metallogenically-enriched crustal regions (metallogenic provinces) may exist that are related to this metasomatised mantle, making their recognition, by isotopic and other means, a worthwhile venture (e.g., Hronsky et al., 2012). Of course, even where such metallogenic provinces exist it may not be related to the presence of metasomatised mantle. For example, as discussed earlier for the Yilgarn Craton and nickel deposits, the topography of the lithosphere-asthenosphere boundary may be just as important (e.g., Begg et al., 2010). The important points here are that there may be a number of reasons why mineralisation may be related to specific lithospheric blocks, and regardless of the actual relationship, datasets such as radiogenic isotopes, may be utilised to identify such blocks and potential metallogenic terranes.

7. Conclusions

Radiogenic isotopes have traditionally been used in detailed mineralisation studies for both geochronological purposes and as tracers. It is also now evident that consideration of such data at regional- and larger scales, e.g., using isotopic maps, can also be used to assist with metallogenic interpretation, including the identification of metallogenic terranes. This approach is being greatly facilitated by the large amounts of isotopic (and other) data becoming increasingly available, in combination with readily available graphical software, which together have made possible construction of such isotopic maps, using various isotopic variables, at regional to continental scales, allowing for metallogenic interpretation over similarly large regions. Such interpretation has also benefited from a mineral systems approach, which recognises that mineral deposits, although geographically small in extent, are the result of geological processes that occur at a variety of scales, up to craton-scale. Examples include identifying lithospheric/crustal architecture and its importance in controlling the locations of mineralisation; the identification of metallogenic terranes and/or favourable geodynamic environments on the basis of their isotopic signatures, as well as identifying metallogenic important rock types by their isotopic signature.

How such isotopic data (and maps) are used depends, to a large degree, on the geochemical specific behaviour of the parent–daughter isotopic systems being used, and the rock types and/ore minerals being analysed. Most current and past focus has been on the Sm–Nd system in felsic igneous rocks and the U–Th–Pb system in galena and Pb-rich associated ores and other rocks. The Sm–Nd system can be used to effectively 'see' through many crustal processes to provide information on the nature of the source of these rocks. For voluminous rocks such as granites this provides a potentially powerful proxy in constraining the nature of the various crustal blocks the granites occur within. In contrast, Pb isotopic data from galena and Pb-rich associated ores provide a more direct link between mineralisation, and various isotopic domains, as delineated by Pb and other (e.g., Sm–Nd) isotopic data, and the two systems can be used in conjunction to investigate links between mineralisation and crustal domains.

Regional and continental scale isotopic maps (and data) using the Sm–Nd and U–Th–Pb systems can be used to empirically and/or predictively to identify and target (either directly or indirectly by proxy), larger scale parts of mineral systems that may be indicative, or form part of, metallogenic terranes, for a variety of mineral systems. These include: demonstrable empirical relationships between mineral systems and isotopic domains, which can be extracted, tested and applied as predictive tools; the identification of old, especially Archean, cratonic blocks, which may be metallogenically-endowed, or have other favourable characteristics; the identification of prior tectonic regimes favourable for mineralisation, e.g., continental margins, especially accretionary orogenic settings,; juvenile zones, either marginal or internal, which may indicate zones of rifting or primitive arc crust; identification of crustal breaks, which may represent fluid pathways for fluids and magmas or serve to delineate natural boundaries for metallogenic terranes; and as baseline maps which help to identify regions/periods characterised by greater (or lesser) magmatic, especially mantle input. Of course, in any exploration model, any analysis is predicated on using a wide range of geological, geochemical and geophysical information across a range of scales. Isotopic maps, such as Sm–Nd and U–Th–Pb images are just another layer to be integrated with other data. Future work should focus on better constraining the 4D (3D plus time) evolution of the whole lithosphere to aid in more effective mineral targeting and exploration. This will involve the use and integration of all available radiogenic isotopic systems, including the voluminous amounts of in situ isotopic analysis (of minerals, in particular Lu–Hf) now available, and incorporation of isotopic data for the mantle lithosphere, especially the Re–Os system.

Acknowledgments

This contribution has benefited from constructive reviews by Michael Doublier and Natalie Kositcin (Geoscience Australia) and journal reviewers Marco Fiorentini and an anonymous reviewer. It is published with permission of the Chief Executive Officer of Geoscience Australia.

References

Ahmad, M., Scrimgeour, I.R., 2013. Geologic Framework. In: Ahmad, M., Minson, T.J. (compilers) Geology and Mineral Resources of the Northern Territory, Northern Territory Geological Survey Special Publication 5.

Arevalo Jr., R., McDonough, W.F., 2010. Chemical variations and regional diversity observed in MORB. Chem. Geol. 271, 70–85.

Arndt, N., 2013. The lithospheric mantle plays no active role in the formation of orthomagmatic ore deposits. Econ. Geol. 108, 1953–1970.

Ayer, J., Amelin, Y., Corfu, F., Kamo, S., Ketchum, J., Kwok, K., Trowell, N., 2002. Evolution of the southern Abitibi greenstone belt based on U–Pb geochronology: autochthonous volcanic construction followed by plutonism, regional deformation and sedimentation. Precambrian Res. 115, 63–95.

Bagas, L., Bierlein, F.P., English, L., Anderson, J.A.C., Maidment, D., Huston, D.L., 2008. An example of a Palaeoproterozoic back-arc basin: Petrology and geochemistry of the ca. 1864 Ma Stubbins Formation as an aid towards an improved understanding of the Granites–Tanami Orogen, Western Australia. Precambrian Res. 166, 168–184.

Barnes, S.J., Fiorentini, M.L., 2010a. Komatiite-hosted nickel sulphide deposits: what's so special about the Kalgoorlie Terrane. In: Tyler, I.M., Knox-Robinson, C.M. (Eds.), Fifth International Archean Symposium Abstracts. Geological Survey of Record 2010/18, pp. 281–283.

Barnes, S.J., Fiorentini, M.L., 2010b. Comparative lithogeochemistry of komatiites in the Eastern Goldfields Superterrane and the Abitibi Greenstone Belt, and implications for distribution of nickel sulphide deposits. In: Wyche, S. (compiler), Yilgarn-Superior workshop-abstracts, Fifth International Archean Symposium 10 September 2010. Geological Survey of Western Australia Record 2010/20, 23–26.

Barnes, S.J., Fiorentini, M.L., 2012. Komatiite magmas and Ni sulfide deposits: a comparison of variably endowed archean terranes. Econ. Geol. 107, 755–780.

Barnicoat, A.C., 2007. Mineral systems and exploration science: linking fundamental controls on ore deposition with the exploration process. In: Andrews, C.J., et al. (Eds.), Digging Deeper. Proceedings of the Ninth Biennial SGA Meeting, Dublin, Ireland, 2007, pp. 1407–1411.

Barrie, C.T., Shirey, S.B., 1991. Nd- and Sr-isotope systematics for the Kamiskotia-Montcalm area: implications for the formation of late Archean crust in the western Abitibi Subprovince, Canada. Can. J. Earth Sci. 28, 58–76.

Beakhouse, G.P., 2007. Gold, granite and Late Archean tectonics: a Superior province perspective. In: Bierlein, F.P., Knox-Robinson, C.M. (Eds.), Proceedings of Geoconferences (WA) Inc. Kalgoorlie'07 Conference, 25–27 September 2007, Kalgoorlie, Western Australia. Geoscience Australia Record 2007/14, pp. 191–195.

Begg, G.C., Griffin, W.L., Natapov, L.M., O'Reilly, S.Y., Grand, S., O'Neill, C.J., Poudjom Djomani, Y., Deen, T., Bowden, P., 2009. The lithospheric architecture of Africa: seismic tomography, mantle petrology and tectonic evolution. Geosphere 5, 23–50.

Begg, G.C., Hronsky, J.A.M., Arndt, N.T., Griffin, W.L., O'Reilly, S.Y., Hayward, N., 2010. Lithospheric, cratonic, and geodynamic setting of Ni–Cu–PGE sulfide deposits. Econ. Geol. 105, 1057–1070.

Bekker, A., Barley, M.E., Fiorentini, M.L., Rouxel, O.J., Rumble, D., Beresford, S.W., 2009. Atmospheric sulphur in Archaean komatiite-hosted nickel deposits. Science 326, 1086–1089.

Belousova, E.A., Kostitsyn, Y.A., Griffin, W.L., Begg, G.C., O'Reilly, S.Y., Pearson, N.J., 2010. The growth of the continental crust: constraints from zircon Hf-isotope data. Lithos 119, 457–466.

Bennett, V.C., DePaolo, D.J., 1987. Proterozoic crustal history of the western United States as determined by neodymium isotopic mapping. Bull. Geol. Soc. Am. 99, 674–685.

Black, L.P., Carr, G.R., Sun, S.-S., 1997. Applied isotope geochronology and geochemistry. In: Bain, J.H.C., Draper, J.J. (Eds.), North Queensland Geology, Australian Geological Survey Organisation Bulletin 240, and Queensland Department of Mines and Energy Queensland. 9, pp. 429–448.

Blevin, P.L., 2004. Redox and compositional parameters for interpreting the granitoid metallogeny of eastern Australia: implications for gold-rich ore systems. Resour. Geol. 54, 241–252.

Blevin, P.L., Chappell, B.W., 1992. The role of magma sources, oxidation states and fractionation in determining the granitoid metallogeny of eastern Australia. Trans. R. Soc. Edinb. Earth Sci. 83, 305–316.

Blevin, P.L., Chappell, B.W., Allen, C.M., 1996. Intrusive metallogenic provinces in eastern Australia based on granite source and composition. Trans. R. Soc. Edinb. Earth Sci. 87, 281–290.

Blewett, R.S., Henson, P.A., Roy, I.G., Champion, D.C., Cassidy, K.F., 2010. Scale integrated architecture of a world-class gold mineral system: the Archaean eastern Yilgarn Craton, Western Australia. Precambrian Res. 183, 230–250.

Browning, P., Groves, D.I., Blockley, J.G., Rosman, K.J.R., 1987. Lead isotope constraints on the age and source of gold mineralization in the Archean Yilgarn block. Econ. Geol. 82, 971–986.

Budd, A.R., 2006. The Tarcoola goldfield of the central Gawler gold province, and the Hiltaba Association Granites, Gawler craton, South Australia. Unpublished Ph.D. thesis, Canberra, ACT, Australian National University, 507 pp.

Campbell, I.H., Compston, D.M., Richards, J.P., Johnson, J.P., Kent, A.J.R., 1998. Review of the application of isotopic studies to the genesis of Cu–Au mineralisation at Olympic Dam and Au mineralisation at Porgera, the Tennant Creek district and Yilgarn Craton. Aust. J. Earth Sci. 45, 201–218.
Carlson, R.W., 2005. Application of the Pt–Re–Os isotopic systems to mantle geochemistry and geochronology. Lithos 82, 249–272.
Carr, G.R., Dean, J.A., Suppel, D.W., Heithersay, P.S., 1995. Precise lead isotope fingerprinting of hydrothermal activity associated with Ordovician to carboniferous metallogenic events in the Lachlan fold belt of New South Wales. Econ. Geol. 90, 1467–1505.
Carr, G.R., Denton, G.J., Korsch, M.J., Gardner, B.L., Parr, J.M., Andrew, A.S., Whitford, D.J., Wyborn, L.A.I., Sun, S.-S., 2001. User friendly isotope technologies in mineral exploration: Pb isotope applications, Northern Australian Proterozoic Basins. CSIRO Report 713C (127 pp.).
Cassidy, K.F., Champion, D.C., 2004. Crustal evolution of the Yilgarn Craton from Nd isotopes and granite geochronology: implications for metallogeny. 33, 317–320.
Cassidy, K.F., Champion, D.C., McNaughton, N.J., Fletcher, I.R., Whitaker, A.J., Bastrakova, I.V., Budd, A.R., 2002. Characterization and metallogenic significance of Archaean granitoids of the Yilgarn Craton. Project P482/MERIWA Project M281, Final Report. Australian Mineral and Industry Research Association, Western Australia, p. 514.
Cassidy, K.F., Champion, D.C., Huston, D.L., 2005. Crustal evolution constraints on the metallogeny of the Yilgarn Craton. In: Mao, J., Bierlein, F.P. (Eds.), Mineral Deposit Research: Meeting the Global Challenge. Springer, Berlin/Heidelberg, pp. 901–904.
Cassidy, K.F., Champion, D.C., Krapež, B., Barley, M.E., Brown, S.J.A., Blewett, R.S., Groenewald, P.B., Tyler, I.M., 2006. A revised geological framework for the Yilgarn Craton. Geological Survey of Report 2006/8 (14 pp.).
Champion, D.C., 2013. Neodymium depleted mantle model age map of Australia: explanatory notes and user guide. Record 2013/044. Geoscience Australia, Canberra (http://dx.doi.org/10.11636/Record.2013.044).
Champion, D.C., Cassidy, K.F., 2007. An overview of the Yilgarn Craton and its crustal evolution. In: Bierlein, F.P., Knox-Robinson, C.M. (Eds.), Proceedings of Geoconferences (WA) Inc. Kalgoorlie'07 Conference, 25–27 September 2007, Kalgoorlie, Western Australia. Geoscience Record 2007/14, pp. 8–13.
Champion, D.C., Cassidy, K.F., 2008. Using geochemistry and isotopic signatures of granites to aid mineral systems studies: an example from the Yilgarn Craton. In: Korsch, R.J., Barnicoat, A.C. (Eds.), 2008. New Perspectives: The Foundations and Future of Australian Exploration. Abstracts for the June 2008 pmd*CRC Conference. Geoscience Australia, Record 2008/09, pp. 7–16.
Champion, D.C., Sheraton, J.W., 1997. Geochemistry and Nd isotope systematics of Archaean granites of the Eastern Goldfields, Yilgarn Craton, Australia; implications for crustal growth processes. Precambrian Res. 83, 109–132.
Champion, D.C., Smithies, R.H., 2000. The geochemistry of the Yule Granitoid Complex, East Pilbara Granite–Greenstone Terrane; evidence for early felsic crust. Geological Survey of Western Australia 1999–2000 Annual Review, pp. 42–48.
Champion, D.C., Smithies, R.H., 2007. Chapter 4.3 Geochemistry of Paleoarchean Granites of the East Pilbara Terrane, Pilbara Craton, Western Australia: Implications for Early Archean Crustal Growth. Developments in Precambrian Geology 15, 369–409.
Champion, D.C., Bultitude, R.J., Blevin, P.L., 2010. Geochemistry and isotope systematics of Carboniferous to Triassic felsic magmatism in northeastern Australia—putting the New England Orogen in its place. In: Buckman, S., Blevin, P.L. (Eds.), New England Orogen 2010. Proceedings of a conference held at the University of New England, Armidale, New South Wales, Australia, November 2010. University of New England, Armidale, pp. 112–118.
Collins, W.J., Belousova, E.A., Kemp, A.I.S., Murphy, J.B., 2011. Two contrasting Phanerozoic orogenic systems revealed by hafnium isotope data. Nat. Geosci. 4, 333–337. http://dx.doi.org/10.1038/NGEO1127.
Cooke, D.R., Wilson, A.J., House, M.J., Wolfe, R.C., Walshe, J.L., Lickfold, V., Crawford, A.J., 2007. Alkalic porphyry Au–Cu and associated mineral deposits of the Ordovician to Early Silurian Macquarie Arc, New South Wales. Aust. J. Earth Sci. 55, 445–463.
Cumming, G.L., Richards, J.R., 1975. Ore lead isotope ratios in a continuously changing earth. Earth Planet. Sci. Lett. 28, 155–171.
Czarnota, K., Champion, D.C., Cassidy, K.F., Goscombe, B., Blewett, R.S., Henson, P.A., Groenewald, P.B., 2010. Late Archaean geodynamic processes: how the Eastern Goldfields Superterrane evolved in time and space. Precambrian Res. 183, 175–202.
DePaolo, D.J., 1981. Neodymium isotopes in the Colorado Front Range and crust–mantle evolution in the Proterozoic. Nature 291, 193–196.
DePaolo, D.J., 1988. Neodymium Isotope Geochemistry: An Introduction. Springer-Verlag, Berlin (187 pp.).
DePaolo, D.J., Wasserburg, G.J., 1976. Nd isotopic variations and petrogenetic models. Geophys. Res. Lett. 3, 249–252.
Dickin, A.P., 1995. Radiogenic Isotope Geology. Cambridge University Press (490 pp.).
Doe, B.R., Zartman, R.E., 1979. Plumbotectonics I, the Phanerozoic. In: Barnes, H.L. (Ed.), Geochemistry of Hydrothermal Ore Deposits. Wiley Interscience, New York, pp. 22–70.
Farmer, G.L., DePaolo, D.J., 1983. Origin of Mesozoic and Tertiary granite in the western United States and implications for pre-Mesozoic crustal structure I. Nd and Sr isotopic studies in the geocline of the northern Great Basin. J. Geophys. Res. 88, 3379–3401.
Farmer, G.L., DePaolo, D.J., 1984. Origin of Mesozoic and Tertiary granite in the western United States and implications for pre-Mesozoic crustal structure II. Nd and Sr isotopic studies of unmineralised and Cu- and Mo-mineralized granite in the Precambrian craton. J. Geophys. Res. 89, 10141–10160.
Faure, G., 1977. Principles of Isotope Geology. Second Edition. John Wiley and Sons, New York (589 pp.).
Ferris, G.M., Schwarz, M., 2004. Definition of the Tunkillia Suite, western Gawler Craton. MESA J. 34, 32–41.
Ferris, G.M., Schwarz, M.P., Heithersay, P., 2002. The geological framework, distribution and controls of Fe-oxide Cu–Au mineralisation in the Gawler Craton, South Australia. Part I—Geological and tectonic framework. In: Porter, T.M. (Ed.)-Hydrothermal Iron Oxide Copper-Gold and Related Deposits: A Global Perspective vol. 2. PGC Publishing, Adelaide, pp. 9–31.
Fiorentini, M.L., Beresford, S.W., Barley, M.E., Duuring, P., Bekker, A., Rosengren, N., Cas, R., Hronsky, J., 2012. District to camp controls on the genesis of komatiite-hosted nickel sulfide deposits, Agnew-Wiluna greenstone belt, Western Australia: insights from the multiple sulfur isotopes. Econ. Geol. 107, 781–796.
Fisher, C.M., Vervoort, J.D., Dufrane, S.A., 2014. Accurate Hf isotope determinations of complex zircons using the "laser ablation split stream" method. Geochem. Geophys. Geosyst. 15, 121–139. http://dx.doi.org/10.1002/2013GC004962.
Franklin, J.M., Gibson, H.L., Jonasson, I.R., Galley, A.G., 2005. Volcanogenic massive sulfide deposits. Economic Geology 100th Anniversary Volume, pp. 523–560.
Goldfarb, R., Santosh, M., 2013. The dilemma of the Jiaodong gold deposits: are they unique? Geosci. Front. http://dx.doi.org/10.1016/j.gsf.2013.11.001.
Goleby, B.R., Huston, D.L., Lyons, P., Vandenberg, L., Bagas, L., Davies, B.M., Jones, L.E.A., Gebre-Mariam, M., Johnson, W., Smith, T., English, L., 2009. The Tanami deep seismic reflection experiment: an insight into gold mineralization and paleoproterozoic collision in the North Australian Craton. Tectonophysics 472, 169–182.
Gregory, M.J., Schaefer, B.F., Keays, R.R., Wilde, A.R., 2008. Rhenium–osmium systematics of the Mount Isa copper orebody and the Eastern Creek Volcanics, Queensland, Australia: implications for ore genesis. Mineral. Deposita 43, 553–573.
Griffin, W.L., Belousova, E.A., Shee, S.R., Pearson, N.J., O'Reilly, S.Y., 2004. Archean crustal evolution in the northern Yilgarn Craton: U–Pb and Hf-isotope evidence from detrital zircons. Precambrian Res. 131, 231–282.
Griffin, W.L., Begg, G.C., O'Reilly, S.Y., 2013. Continental-root control on the genesis of magmatic ore deposits. Nat. Geosci. 6, 905–910. http://dx.doi.org/10.1038/NGEO1954.
Groves, D.I., Batt, W.D., 1984. Spatial and temporal variations of archaean metallogenic associations in terms of evolution of granitoid-greenstone terrains with particular emphasis on the Western Australian shield. In: Kroner, A., Hanson, G.N., Goodwin, A.M. (Eds.), Archaean Geochemistry. Springer-Verlag, Berlin, pp. 73–98.
Groves, D.I., Bierlein, F.P., Meinert, L.D., Hitzman, M.W., 2010. Iron oxide copper-gold (IOCG) deposits through earth history: implications for origin, lithospheric setting, and distinction from other epigenetic iron oxide deposits. Econ. Geol. 105, 641–654.
Hart, T.R., Gibson, H.L., Lesher, C.M., 2004. Trace element geochemistry and petrogenesis of felsic volcanic rocks associated with volcanogenic massive Cu–Zn–Pb sulfide deposits. Econ. Geol. 99, 1003–1013.
Henderson, R.A., Innes, B.M., Fergusson, C.L., Crawford, A.J., Withnall, I.W., 2011. Collisional accretion of a Late Ordovician oceanic island arc, northern Tasman Orogenic Zone, Australia. Aust. J. Earth Sci. 58, 1–19.
Hergt, J.M., Chappell, B.W., McCulloch, M.T., McDougall, I., Chivas, A.R., 1989. Geochemical and isotopic constraints on the origin of the Jurassic dolerites of Tasmania. J. Petrol. 30, 841–883.
Hronsky, J.M.A., Groves, D.I., Loucks, R.R., Begg, G.C., 2012. A unified model for gold mineralisation in accretionary orogens and implications for regional-scale exploration targeting methods. Mineral. Deposita 47, 339–358.
Hussey, K.J., Huston, D.L., Claoué-Long, J.C., 2005. Geology and origin of some CU–Pb–Zn (Au–Ag) deposits in the Strangways Metamorphic Complex, Arunta Region. Geological Survey Report 17.
Huston, D.L., Sun, S.-S., Blewett, R., Hickman, A.H., Van Kranendonk, M., Phillips, D., Baker, D., Brauhart, C., 2002. The timing of mineralization in the Archean North Pilbara Terrain, Western Australia. Econ. Geol. 97, 733–755.
Huston, D.L., Champion, D.C., Cassidy, K.F., 2005. Tectonic controls on the endowment of Archean cratons in VHMS deposits: evidence from Pb and Nd isotopes. In: Mao, J., Bierlein, F.P. (Eds.), Mineral Deposit Research: Meeting the Global Challenge. Springer, Berlin/Heidelberg, pp. 15–18.
Huston, D.L., Blewett, R.S., Champion, D.C., 2012. Australia through time: a summary of its tectonic and metallogenic evolution. Episodes 35, 23–43.
Huston, D.L., Champion, D.C., Cassidy, K.F., 2014. Tectonic controls on the endowment of neoarchean cratons in volcanic-hosted massive sulfide deposits: evidence from lead and neodymium isotopes. Econ. Geol. 109, 11–26. http://dx.doi.org/10.2113/econgeo.109.1.11.
Huston, D.L., Mernagh, T.P., Hagemann, S.G., Doublier, M.P., Fiorentini, M., Champion, D.C., Jaques, A.L., Czarnota, K., Ross Cayley, R., Skirrow, R., Bastrakov, E., 2016. Tectono-metallogenic systems—the place of mineral systems within tectonic evolution. Ore Geol. Rev. 76, 168–210 (in this volume).
Ishihara, S., 1977. The magnetite-series and ilmenite-series granitic rocks. J. Min. Geol. 27, 293–305.
Ishihara, S., 1981. The granitoid series and mineralization. Economic Geology 75th Anniversary volume, pp. 458–484.
Jégo, S., Pichavant, M., Mavrogenes, J.A., 2010. Controls on gold solubility in arc magmas: an experimental study at 1000 °C and 4 kbar. Geochim. Cosmochim. Acta 74, 2165–2189.
Johnson, J.P., McCulloch, M.T., 1995. Sources of mineralising fluids for the Olympic Dam deposit (South Australia): Sm–Nd isotopic constraints. Chem. Geol. 121, 177–199.
Kamenov, G., Macfarlane, A.W., Riciputi, L., 2002. Sources of lead in the San Cristobal, Pulacayo, and Potosí Mining Districts, Bolivia, and a reevaluation of regional ore lead isotope provinces. Econ. Geol. 97, 573–592.
Kemp, A.I.S., Hawkesworth, C.J., Foster, G.L., Paterson, B.A., Woodhead, J.D., Hergt, J.M., Gray, C.M., Whitehouse, M.J., 2007. Magmatic and crustal differentiation history of granitic rocks from Hf–O isotopes in zircon. Science 315, 980–983.
Kemp, A.I.S., Hawkesworth, C.J., Collins, W.J., Gray, C.M., Blevin, P.L., EIMF, 2009. Isotopic evidence for rapid continental growth in an extensional accretionary orogen: the Tasmanides, eastern Australia. Earth Planet. Sci. Lett. 284, 455–466.

Kennett, B.L.N., Salmon, M., 2012. AuSREM: Australian seismological reference model. Aust. J. Earth Sci. 59, 1091–1103. http://dx.doi.org/10.1080/08120099.2012.736406.
Kennett, B.L.N., Fichtner, A., Fishwick, S., Yoshizawa, K., 2013. Australian seismological reference model (AuSREM): mantle component. Geophys. J. Int. 192, 871–887. http://dx.doi.org/10.1093/gji/ggs065.
Ketchum, J.W.F., Ayer, J.A., van Breemen, O., Pearson, N.J., Becker, J.K., 2008. Pericontinental crustal growth of the southwestern Abitibi Subprovince, Canada—UPb, Hf, and Nd isotope evidence. Econ. Geol. 103, 1151–1184.
Korsch, R.J., Doublier, M.P., 2016. Major crustal boundaries of Australia and their significance in mineral systems targeting. Ore Geol. Rev. 76, 211–228 (in this volume).
Korsch, R.J., Kositcin, N., Champion, D.C., 2011. Australian island arcs through time: geodynamic implications for the Archean and Proterozoic. Gondwana Res. 19, 716–734.
Kositcin, N., Champion, D.C., Huston, D.L., 2009. Geodynamic synthesis of the north Queensland region and implications for metallogeny. Geoscience Record 2009/30 (196 pp.).
Krapez, B., Brown, S.J.A., Hand, J., Barley, M.E., Cas, R.A.F., 2000. Age constraints on recycled crustal and supracrustal sources of Archaean metasedimentary sequences, Eastern Goldfields Province, Western Australia: evidence from SHRIMP zircon dating. Tectonophysics 322, 89–133.
Lambert, D.D., Foster, J.G., Frick, L.R., Ripley, E.M., 1999. Re–Os isotope geochemistry of magmatic sulphide ore systems. In: Lambert, D.D., Ruiz, J. (Eds.), Application of Radiogenic Isotopes to ore Deposit Research and Exploration. 12, pp. 29–58.
Lang, J.R., Baker, T., Hart, C.J.R., Mortensen, J.K., 2000. An exploration model for intrusion-related gold systems. Society of Economic Geology Newsletter 40.
Lesher, C.M., Goodwin, A.M., Campbell, I.H., Gorton, M.P., 1986. Trace-element geochemistry of ore-associated and barren, felsic metavolcanic rocks in the superior province, Canada. Can. J. Earth Sci. 23, 222–237.
Liew, T.C., McCulloch, M.T., 1985. Genesis of granitoid batholiths of Peninsular Malaysia and implications for models of crustal evolution: evidence from a Nd–Sr isotopic and U–Pb, zircon study. Geochim. Cosmochim. Acta 49, 587–600.
Macfarlane, A.W., Marcet, P., LeHuray, A.P., Petersen, U., 1990. Lead isotope provinces of central Andes inferred from ores and crustal rocks. Econ. Geol. 85, 1857–1880.
Magoon, L.B., Dow, W.G., 1994. The petroleum system. In: Magoon, L.B., Dow, W.G. (Eds.), The Petroleum System: From Source to Trap. American Association of Petroleum Geologists Memoir 60, pp. 3–24.
McCuaig, T.C., Beresford, S., Hronsky, J., 2010. Translating the mineral systems approach into an effective exploration targeting system. Ore Geol. Rev. 38, 128–138.
McCulloch, M.T., 1987. Sm–Nd isotopic constraints on the evolution of Precambrian crust in the Australian continent. In: Kroner, A. (Ed.), Proterozoic lithospheric evolution. American Geophysical Union Geodynamics Series vol. 17.
McCulloch, M.T., Wasserburg, G.J., 1978. Sm–Nd and Rb–Sr chronology of continental crust formation. Science 200, 1003–1011.
McDonald, G.D., Collerson, K.D., Kinny, P.D., 1997. Late Archean and Early Proterozoic crustal evolution of the Mount Isa Block, northwest Queensland, Australia. Geology 25 (12), 1095–1098.
McDonough, W.F., 2003. Compositional model for the earth's core. In: Holland, H.D., Turekian, K.K. (Eds.), Treatise on Geochemistry, Volume 2, The Mantle and Core. Elsevier, New York, pp. 547–568.
McDonough, W.F., Sun, S.-S., 1995. Composition of the Earth. Chem. Geol. 120, 223–253.
McNaughton, N.J., Cassidy, K.F., Dahl, N., Groves, D.I., Perring, C.S., Sang, J.H., 1990. Lead isotope studies. In: Ho, S.E., Groves, D.I., Bennett, J.M. (Eds.), Gold Deposits of the Archaean Yilgarn Block, Western Australia: Nature, Genesis and Exploration Guidelines: Geology Department (Key Centre) & University Extension 20. The University of Western Australia Publication, pp. 395–407.
Mercier-Langevin, P., Dubé, B., Hannington, M.D., Richer-Laflèche, M., Gosselin, G., 2007. The LaRonde Penna Au-rich volcanogenic massive sulfide deposit, Abitibi greenstone belt, Québec: Part II. Lithogeochemistry and paleotectonic setting. Econ. Geol. 102, 611–631.
Mole, D.R., Fiorentini, M.L., Thebaud, N., McCuaig, T.C., Cassidy, K.F., Kirkland, C.L., Wingate, M.T.D., Romano, S.S., Doublier, M.P., Belousova, E.A., 2012. Spatio-temporal constraints on lithospheric development in the southwest-central Yilgarn Craton, Western Australia. Aust. J. Earth Sci. 59, 625–656.
Mole, D.R., Fiorentini, M.L., Cassidy, K.F., Kirkland, C.L., Thebaud, N., McCuaig, T.C., Doublier, M.P., Duuring, M.L., Romano, S.S., Maas, E.A., Belousova, E.A., Barnes, S.J., Miller, J., 2013. Crustal evolution, intra-cratonic architecture and the metallogeny of an Archaean craton. Geological Society of London Special Publications 393 http://dx.doi.org/10.1144/SP393.8 (first published on December 3, 2013).
Mole, D.R., Fiorentini, M.L., Thebaud, N., Cassidy, K.F., McCuaig, T.C., Kirkland, C.L., Romano, S.S., Doublier, M.P., Belousova, E.A., Barnes, S.J., Miller, J., 2014. Archean komatiite volcanism controlled by the evolution of early continents. Proc. Natl. Acad. Sci. 111, 10083–10088. http://dx.doi.org/10.1073/pnas.1400273111.
Morand, V.J., 1993. Stratigraphy and tectonic setting of the Calliope Volcanic Assemblage, Rockhampton area, Queensland. Aust. J. Earth Sci. 40, 15–30.
Murgulov, V., Beyer, E., Griffin, W.L., O'Reilly, S.Y., Walters, S.G., Stephens, D., 2007. Crustal evolution in the Georgetown Inlier, North Queensland, Australia: a detrital zircon grain study. Chem. Geol. 245, 198–218.
Murray, C.G., Blake, P.R., 2005. Geochemical discrimination of tectonic setting for Devonian basalts of the Yarrol Province of the New England orogen, central coastal Queensland: an empirical approach. Aust. J. Earth Sci. 52, 993–1034.
Ojala, V., McNaughton, N.J., Ridley, J.R., Groves, D.I., Fanning, C.M., 1997. The Archaean Granny Smith gold deposit, Western Australia: age and Pb-isotope tracer studies. Chronique de la Recherche Minière 529, pp. 75–89.
O'Reilly, S.Y., Griffin, W.L., 2006. Imaging global chemical and thermal heterogeneity in the subcontinental lithospheric mantle with garnets and xenoliths: geophysical implications. Tectonophysics 416, 289–309.
Palme, H., Jones, A., 2003. Solar system abundances of the elements. In: Holland, H.D., Turekian, K.K. (Eds.), Treatise on Geochemistry, Volume 1, Meteorites, comets and planets. Elsevier, New York, pp. 41–61.
Parkinson, I.J., Arculus, R.J., 1999. The redox state of subduction zones: insights from arc-peridotites. Chem. Geol. 160, 409–423.
Payne, J.L., Hand, M., Barovich, K.M., Reid, A., Evans, D.A.D., 2009. Correlations and reconstruction models for the 2500–1500 Ma evolution of the Mawson Continent. In: Reddy, S.M., Mazumder, R., Evans, D.A.D., Collins, A.S. (Eds.), Palaeoproterozoic supercontinents and global evolution. 323, pp. 319–355.
Payne, J.L., Ferris, G., Barovich, K.M., Hand, M., 2010. Pitfalls of classifying ancient magmatic suites with tectonic discrimination diagrams: an example from the Paleoproterozoic Tunkillia Suite, southern Australia. Precambrian Res. 177, 227–240.
Pearson, D.G., Carlson, R.W., Shirey, S.B., Boyd, F.R., Nixon, P.H., 1995. Stabilisation of Archaean lithospheric mantle: a Re-Os isotope study of peridotite xenoliths from the Kaapvaal craton. Earth Planet. Sci. Lett. 134, 341–357.
Polat, A., Kerrich, R., 2002. Nd-isotope systematics of ~2.7 Ga adakites, magnesian andesites, and arc basalts, Superior Province, Canada: evidence for shallow crustal recycling at Archean subduction zones. Earth Planet. Sci. Lett. 202, 345–360.
Price, R.C., Nicholls, I.A., Day, A., 2014. Lithospheric influences on magma compositions of late Mesozoic and Cenozoic intraplate basalts (the Older Volcanics) of Victoria, southeastern Australia. Lithos 206-207, 179–200.
Priestley, K., MacKenzie, D., 2013. The relationship between shear wave velocity, temperature, attenuation and viscosity in the shallow part of the mantle. Earth Planet. Sci. Lett. 381, 78–91.
Prior, G.J., Gibson, H.L., Watkinson, D.H., Cousens, B.L., Cook, R.E., Barrie, C.T., 1999. Sm–Nd isotope study of rhyolites from the Kidd Creek mine area, Abitibi Subprovince, Canada. Econ. Geol. Monogr. 10, 485–496.
Reid, A.J., Hand, M., 2012. Mesoarchean to mesoproterozoic evolution of the southern Gawler cratOn, South Australia. Episodes 35, 216–225.
Rowe, M.C., Kent, A.J.R., Nielsen, R.L., 2009. Subduction influence on oxygen fugacity and trace and volatile elements in basalts across the Cascade volcanic arc. J. Petrol. 50, 61–91.
Rudnick, R.L., Gao, S., 2004. Composition of the continental crust. In: Holland, H.D., Turekian, K.K. (Eds.), Treatise on Geochemistry, volume 3, The Crust. Elsevier, New York, pp. 1–64.
Ruiz, J., Mathur, R., 1999. Metallogenesis in continental margins: Re–Os evidence from porphyry copper deposits in Chile. In: Lambert, D.D., Ruiz, J. (Eds.), Application of Radiogenic Isotopes to ore Deposit Research and Exploration. 12, pp. 59–72.
Salier, B.P., 2004. The timing and source of gold bearing fluids in the Laverton greenstone belt, Yilgarn Craton, Western Australia. Unpublished Ph.D. thesis, University of Western Australia, Perth, 379 pp.
Salters, V.J.M., Stracke, A., 2004. Composition of the depleted mantle. Geochem. Geophys. Geosyst. 5, Q05B07. http://dx.doi.org/10.1029/2003GC000597.
Scrimgeour, I.R., Kinny, P.D., Close, D.F., Edgoose, C.J., 2005. High-T granulites and polymetamorphism in the southern Arunta region, central Australia: evidence for a 1.64 Ga accretional event. Precambrian Res. 142, 1–27.
Shirey, S.B., Walker, R.J., 1998. The Re-os system in cosmochemistry and high-temperature geochemistry. Annu. Rev. Earth Planet. Sci. 26, 423–500.
Sircombe, K.N., 1999. Tracing provenance through the isotope ages of littoral and sedimentary detrital zircon, eastern Australia. Sediment. Geol. 124, 47–67.
Skirrow, R.G., 2010. "Hematite-Group" IOCG ± U ore systems: tectonic settings, hydrothermal characteristics, and Cu–Au and U mineralizing processes. In: Corriveau, L., Mumin, H. (Eds.), Exploring for Iron Oxide Copper-Gold (Ag-Bi-Co-U) Deposits. Examples from Canada and global analogues. Geological Association of Canada Short Course Notes 20, pp. 39–58.
Skirrow, R.G., 2013. Australia's iron oxide Cu–Au provinces: world-class opportunities. Presentation given at Prospectors and Developers Association of (PDAC) Convention, Toronto 36 March 2013.
Skirrow, R.G., Bastrakov, E.N., Barovich, K., Fraser, G.L., Creaser, R.A., Fanning, C.M., Raymond, O.L., Davidson, G.J., 2007. Timing of iron oxide Cu–Au-(U) hydrothermal activity and Nd isotope constraints on metal sources in the Gawler Craton, South Australia. Econ. Geol. 102, 1441–1470.
Slocum, T.A., McMaster, R.B., Kessler, F.C., Howard, H.H., 2009. Thematic Cartography and Geovisualization. Third Edition. Pearson Prentice Hall, New Jersey (561 pp.).
Smithies, R.H., Champion, D.C., 2000. The Archaean high-Mg diorite suite: links to tonalite–trondhjemite–granodiorite magmatism and implications for early Archaean crustal growth. J. Petrol. 41, 1653–1671.
Smithies, R.H., Champion, D.C.V., Kranendonk, M.J., Howard, H.M., Hickman, A.H., 2005. Modern-style subduction processes in the Mesoarchaean: geochemical evidence from the 3.12 Ga Whundo intra-oceanic arc. Earth Planet. Sci. Lett. 231, 221–237.
Söderlund, U., Patchett, P.J., Vervoort, J.D., Isachsen, C.E., 2004. The ^{176}Lu decay constant determined by Lu–Hf and U–Pb isotope systematics of Precambrian mafic intrusions. Earth Planet. Sci. Lett. 219, 311–324.
Stacey, J.S., Kramer, J.D., 1975. Approximation of terrestrial lead isotope evolution by a two stage model. Earth Planet. Sci. Lett. 26, 207–221.
Stern, R.A., 1999. Insitu analysis of radiogenic isotopes with emphasis on ion microprobe techniques and applications. In: Lambert, D.D., Ruiz, J. (Eds.), Application of Radiogenic Isotopes to ore Deposit Research and Exploration. 12, pp. 173–199.
Stewart, A.J., Raymond, O.L., Totterdell, J.M., Zhang, W., Gallagher, R., 2013. Australian Geological Provinces, 2013.01 edition. 2013.01 ed. Scale 1:2500000. Geoscience Australia, Canberra, Australia.
Sun, S.-S., McDonough, W.F., 1989. Chemical and isotopic systematics of oceanic basalts: implications for mantle composition and processes. In: Saunders, A.D., Norry, M.J. (Eds.), Magmatism in the Ocean Basins. Geological Society of London Special Publication 42, pp. 313–345.
Sun, S.-S., Warren, R.G., Shaw, R.D., 1995. Nd isotope study of granites from the Arunta Inlier, central Australia: constraints on geological models and limitation of the method. Precambrian Res. 71, 301–314.
Sun, S.-S., Carr, G.R., Page, R.W., 1996. A continued effort to improve lead-isotope model ages: AGSO Research Newsletter 24, 19–20.

Swain, G., Woodhouse, A., Handa, M., Barovich, K., Schwarz, M., Fanning, C.M., 2005. Provenance and tectonic development of the late Archaean Gawler Craton, Australia; U–Pb zircon, geochemical and Sm–Nd isotopic implications. Precambrian Res. 141, 106–136.

Swain, G., Barovich, K., Hand, M., Ferris, G., Schwarz, M., 2008. Petrogenesis of the St Peter Suite, southern Australia: arc magmatism and Proterozoic crustal growth of the South Australian Craton. Precambrian Res. 166, 283–296.

Thompson, J.F.H., Sillitoe, R.H., Baker, T., Lang, J.R., Mortensen, J.K., 1999. Intrusion-related gold deposits associated with tungsten-tin provinces. Mineral. Deposita 34, 323–334.

Thorpe, R.I., 1999. The Pb isotope linear array for volcanogenic massive sulfides deposits of the Abitibi and Wawa Subprovinces, Canadian Shield. Econ. Geol. Monogr. 10, 555–576.

Thorpe, R.I., Hickman, A.H., Davis, D.W., Mortensen, J.K., Trendall, A.F., 1992. Constraints to models for Archean lead evolution from precise zircon U–Pb geochronology for the Marble Bar Region, Pilbara Craton, Western Australia. In: Glover, J.E., Ho, S.E. (Eds.), The Archaean; terrains, processes and metallogeny; proceedings volume for the Third international Archaean symposium. Geology Department (Key Centre) & University Extension, The University of Western Australia Publication 22, pp. 395–407.

Tosdal, R.M., Wooden, J.L., Bouse, R.M., 1999. Pb Isotopes, ore Deposits and Metallogenic Terranes. In: Lambert, D.D., Ruiz, J. (Eds.), Application of Radiogenic Isotopes to ore Deposit Research and Exploration. 12, pp. 1–28.

Valley, J.W., Lackey, J.S., Cavosie, A.J., Clechenko, C.C., Spicuzza, M.J., Basei, M.A.S., Bindeman, I.N., Ferreira, V.P., Sial, A.N., King, E.M., Peck, W.H., Sinha, A.K., Wei, C.S., 2005. 4.4 billion years of crustal maturation: oxygen isotope ratios of magmatic zircon. Contrib. Mineral. Petrol. 150, 561–580.

Van Kranendonk, M.J., Smithies, R.H., Hickman, A.H., Champion, D.C., 2007. Paleoarchean development of a continental nucleus: the East Pilbara Terrane of the Pilbara Craton, Western Australia. In: Van Kranendonk, M.J., Smithies, R.H., Bennett, V.C. (Eds.), Earth's Oldest Rocks. Developments in Precambrian Geology vol. 15. Elsevier, pp. 307–337.

Vervoot, J.D., White, W.M., Thorpe, R.I., 1994. Nd and Pb isotope ratios of the Abitibi greenstone belt: new evidence for very early differentiation of the earth. Earth Planet. Sci. Lett. 128, 215–229.

Warren, R.G., Thorpe, R.I., Dean, J.A., Mortensen, J.K., 1995. Pb-isotope data from base-metal deposits in central Australia: implications for Proterozoic stratigraphic correlations. AGSO J. Aust. Geol. Geophys. 15, 501–509.

Wooden, J.L., Kistler, R.W., Tosdal, R.M., 1998. Pb isotopic mapping of crustal structure in the northern Great Basin and relationships to Au deposit trends. In: Tosdal, R.M. (Ed.), Contributions to the Gold Metallogeny of Northern Nevada, United States Geological Survey Open-File Report, pp. 98–338.

Wyborn, L.A.I., 1997. Australian mineral systems; a National Geoscience Mapping Accord Project. Australian Geological Survey Organisation Record 1997/56.

Wyborn, L.A.I., Heinrich, C.A., Jaques, A.L., 1994. Australian Proterozoic mineral systems: essential ingredients and mappable criteria. Conference proceeedings 1994 AusIMM annual conference, Darwin, August 1994. AusIMM Publication Series 5/94, pp. 109–115.

Xue, Y., Campbell, I., Ireland, T.R., Holden, P., Armstrong, R., 2013. No mass-independent sulfur isotope fractionation in auriferous fluids supports a magmatic origin for Archean gold deposits. Geology 41, 791–794.

Zartman, R.E., 1974. Lead isotopic provinces in the cordillera of the western United States and their geologic significance. Econ. Geol. 69, 792–805.

Zartman, R.E., Doe, B.R., 1981. Plumbotectonics – the model. Tectonophysics 75, 135–162.

Zhang, M., O'Reilly, S.A., Wang, K.-L., Hronsky, J., Griffin, W.L., 2008. Flood basalts and metallogeny: the lithospheric mantle connection. Earth-Sci. Rev. 86, 145–174.

Zhao, J., McCulloch, M.T., 1995. Geochemical and Nd isotopic systematics of granites from the Arunta Inlier, central Australia: implications for Proterozoic crustal evolution. Precambrian Res. 71, 265–299.

Zindler, A., Hart, S., 1986. Chemical geodynamics. Annu. Rev. Earth Planet. Sci. 14, 493–571.